TVVR 15/5016

Spatial variation of infiltration properties in Paria, Oruro, Bolivia

Martin Rosén

Master thesis

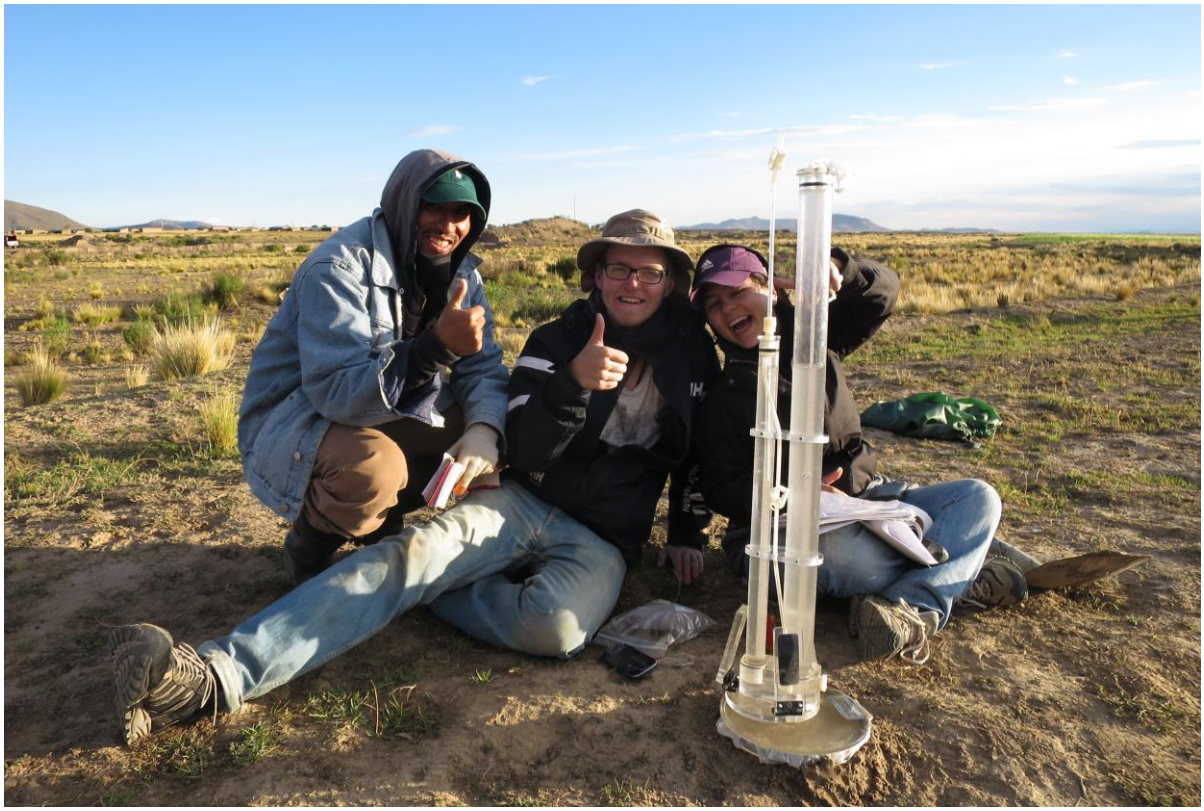

Department of Water Resources

Supervisor: Gerhard Barmen Co-supervisors: Claudia Canedo, Etzar Gomez, Ramiro Simòn Examinator: Ronny Berndtsson

Spatial variation of infiltration properties in Paria, Oruro, Bolivia

Martin Rosén

Department of water resources
TVVR 15/5016
ISSN 1101-9824

Lund 2015
www.tvrl.lth.se

Cover photo: First successful measurement with the infiltrometer. To the left Etzar Gomez, middle Martin Rosén, right Claudia Canedo. Photo Mauricio Gomez

Abstract

Water is necessary for all life and one of the most important natural resources. The water resources problems were the reason why the project *Development of the Altiplano area in Bolivia: a collaboration between Lund University (Sweden) and San Andres University in La Paz (Bolivia)* was started. In the project PhD students are investigating the groundwater aquifer Challapampa that supplies the city of Oruro with water. Part of the project is performing a water balance on the groundwater aquifer and includes gathering of infiltration data. To collect infiltration data is a tedious activity thus it is important to investigate ways to relate infiltration properties of a soil to other parameters and by that reduce the requirement of infiltration data.

The study addresses the possibilities of decreasing the amount of required infiltration data by investigating relationships between soil parameters e.g. moisture content and hydraulic conductivity. It was realized by studying 91 locations covering an area of around 60 times 60 meters in the village of Paria northeast of the city Oruro, located on the Challapampa aquifer. The study investigates infiltration using a tension disc infiltrometer and soil moisture content at depths of 0-10cm and 10-20cm. The analysis with the tension disc infiltrometer was performed with tensions -100 mm and -50 mm and the data were analyzed using three different methods; developed by Ankeny, et al(1991) and Zhang (1998). In addition the differentiated linearization, developed by Vandervaere et al(2000), was used in conjunction with Zhang (1998). The negative results were discarded because negative results do not have physical meaning according to Vandervaere et al (2000). The data were analyzed in ESRI ArcGIS to produce maps describing the spatial variation of the results. Several different interpolation methods were tested.

The amount of negative, and therefore discarded, results accounted for 22% using the constant infiltration rate method by Ankeny et al(1991), 36% for Zhang (1998) and 38% for Zhang (1998) with differentiated linearization. The hydraulic conductivities at the top section of the soil layers were in the range $[10^{-7}\text{-}10^{-5}]ms^{-1}$ with a mean of $[2.0\text{-}2.8]10^{-6}ms^{-1}$ for tension h=-100mm and a mean of $[5.8 - 5.9]10^{-6}\ ms^{-1}$ for tension h=-50mm. The soil moisture content was in the range of 0.6-50.7% with a mean of 6.6% for 0-10cm depth and [2.1-13.6]% with a mean of 6.5% for 10-20cm depth. The kriging interpolation method was found to be the most suitable due to very high or low results at the borders using other methods.

No clear relationships between hydraulic conductivity and soil moisture content were found.

Investigation of the physical processes for infiltration should continue so that better instruments or methods could be developed. Also research on substitutes for infiltration should continue because it can create faster measurements with already existing methods and equipment. Furthermore the investigation on the water availability of the Altiplano should continue, including efforts to connect previous studies to new and to make unavailable studies available to the public.

Keywords
Tension infiltrometer, spatial analysis, hydraulic conductivity, Altiplano, Oruro

LUNDS TEKNISKA HÖGSKOLA
Lunds universitet

Lund University
Faculty of Engineering, LTH
Departments of Earth and Water Engineering

This study has been carried out within the framework of the Minor Field Studies (MFS) Scholarship Programme, which is funded by the Swedish International Development Cooperation Agency, Sida.

The MFS Scholarship Programme offers Swedish university students an opportunity to carry out two months' field work in a developing country resulting in a graduation thesis work, a Master's dissertation or a similar in-depth study. These studies are primarily conducted within subject areas that are important from an international development perspective and in a country supported by Swedish international development assistance.

The main purpose of the MFS Programme is to enhance Swedish university students' knowledge and understanding of developing countries and their problems. An MFS should provide the student with initial experience of conditions in such a country. A further purpose is to widen the human resource base for recruitment into international co-operation. Further information can be reached at the following internet address: http://www.tg.lth.se/mfs

The responsibility for the accuracy of the information presented in this MFS report rests entirely with the authors and their supervisors.

Gerhard Barmen

Gerhard Barmen
Local MFS Programme Officer

Postadress Box 118, 221 00 Lund *Besöksadress* John Ericssons väg 1 *Telefon dir* 046-222 9657, *växel* 046-222 00 00 *Telefax* 046-2229127
E-post Gerhard.Barmen@tg.lth.se

Aknowledgements

There are many people I wish to thank for making the project possible. First, I would like to thank Escuela Runawasi language school and the Ayala family in Cochabamba for teaching me Spanish and helping me with many practicalities. In Oruro, I stayed at the house of Elba and Liset and I am forever thankful for their help and caring. I also got the opportunity to know Gonzalo who taught me about the folk music of Bolivia and to play the instrument charango.

While performing my study I received help from PhD students Etzar Gomez and Claudia Canedo and I thank them for being great supervisors and helping me with many practicalities. During the fieldwork I received help from students Maurcio Garcia and Stephanie Flor Zarate Lima and the fieldwork would have taken much longer time and been much lonelier without them. Thank you University Major San Andrès, La Paz for helping with the soil analysis and some practicalities.

Thank you supervisor Gerhard Barmen and examinator Ronny Berndtsson for helping me finish the thesis.

Thank you my family and friends for helping and inspiring me when I needed it the most.

Last but not least thank you SIDA (Swedish foreign aid authority) for making this project possible through your scholarship.

Thank you everyone! Picture on upper left: The first successful measurement, with Claudia Canedo and Etzar Gomez. Picture on upper right: students Stephanie Flor Zarate Lima and Mauricio Garcia. Picture on lower left: the Ayala family. Picture on lower right: Liset.

List of abbreviations

Altiplano	Bolivian highland area
K1	Hydraulic conductivity at tension 1 where h=-100 mm
K2	Hydraulic conductivity at tension 2 where h=-50 mm
K1I	Hydraulic conductivity at tension 1 calculated with Method I
K2I	Hydraulic conductivity at tension 2 calculated with Method I
K0I	Hydraulic conductivity at tension h=0 calculated with Method I
K1II	Hydraulic conductivity at tension 1, calculated with Method II
K2II	Hydraulic conductivity at tension 2, calculated with Method II
K1III	Hydraulic conductivity at tension 1, calculated with Method III
K2III	Hydraulic conductivity at tension 2, calculated with Method III

Table of contents

Introduction

Water is necessary for all life and therefore one of the most important natural resources. However due to various reasons many people live in areas with small amounts of water, or water with low quality. Many of these problems arise due to human activities in cities, factories or mines cause different types of contamination. However by addressing these problems human display signs of resilience and adaptability to survive difficult conditions.

The problems with water scarcity are aggravated by climate change which is causing more extreme weather with both more flooding and drought (IPCC, 2014). One of the countries that have problems with both water scarcity and quality is Bolivia (Oxfam International, 2009 and Escuela runawasi, language and culture school, 2015). These problems are expected to increase in the future due to climate change (Oxfam International, 2009). The issue is even further aggravated by the fact that the water related data in Bolivia is scarce. It makes it difficult to predict what will happen with the water in the future (Gomez, 2014). The difficulties with prediction of climate is not a problem solely for Bolivia but also countries such as Sweden, with decent rainfall data from around 1860, has this problem (SMHI, 2015).

Fortunately there are projects to increase the understanding and available data on water resources in Bolivia. One of these projects is *Development of the Altiplano area in Bolivia: a collaboration between Lund University, Sweden and San Andres University in La Paz, Bolivia*. In the project, PhD students Etzar Gomez and Claudia Canedo, from Lund University and Universidad Major de San Andrès, La Paz, are investigating the water resources situation for Oruro.

One important part of the project is to make a water balance of the area. A part of the water balance is data on infiltration properties which can be gathered with infiltration experiments. However infiltration experiments are difficult and time consuming as each measurement usually take up to 90 minutes (Kirkham, 2005). Even more time is necessary if the hydraulic conductivity is low (Zhang, 1998). This master thesis addresses some of the difficulties of doing these infiltration measurements and because these analyzes require many measurements, a large dataset will be generated. This dataset will be used by PhD students Etzar Gomez and Claudia Canedo in their water balance model (Schosinsky & Losilla, 2000). Another important aspect is to compare the data with results of the bachelor thesis by Stephanie Flor Zarate Lima at Universidad Técnica de Oruro. She is also investigating infiltration in the same area in order to make a water balance. Her study was not finished at the time of this report.

Delimitations and assumptions

The following delimitations and assumptions were used in the study. Some are

- The duration of the field work was 2 months.
- Only soil moisture content and hydraulic conductivities of the top soil layers at two tensions were measured
- The study was restricted to the study area described
- The study area was assumed to be completely flat, i.e. no slope
- The total amount of measurement points were 105
- The total amount of soil samples were 440

Purpose

The main purpose of this study was to investigate the spatial variation of infiltration properties in the Bolivian highlands. The properties to be studied are the hydraulic conductivities at different tensions and the relationship between the hydraulic conductivity and soil moisture content. The location of the study was at Paria River outside the city Oruro, Bolivia.

Question formulations

The following research questions were formulated:

- Is there any connection between hydraulic conductivities at different tensions and soil moisture content?
- How does the hydraulic conductivity and soil moisture content vary spatially?
- Which method of analyzing the data from tension infiltrometer is the most useful?
- In which range does the hydraulic conductivities at different tensions vary?

Background

Bolivia

Bolivia is a country in central South America with 10 million inhabitants and an area of 1,098,581 square km, more than double the size of Sweden (CIA, 2015). Bolivia has 36 official cultures and languages, most notably Quechua, the remnants of Inca, and Aymara. However, Spanish is the language used by most people and it is the language used by officials. The capital is Sucre, with the government situated in La Paz.

Bolivia is situated in the tropical region but the climate varies significantly across the country due to very large variations of altitude, which stretches from almost sea level in the Amazonian basin to peaks above 6000 meters in the Andes (Wikipedia, 2014). The Andes divides the country roughly into a highland part, the Altiplano which covers one third of the country and a lush lowland part, covering two thirds. The variation in altitude creates an immense biodiversity.

Most of the modern history is concentrated rich mineral deposits such as silver and tin which have been mined in e.g. Potosi and Oruro for over 400 years (Mesa Gisbert et al, 2012). While these minerals are in decline, large deposits of lithium create new opportunities (Svenska Dagbladet, 2009). Bolivia has a complicated relationship with the coca plant: while being a cultural plant used for millennials in tea or chewed to combat fatigue and altitude sickness, Bolivia remains one of the largest producers of cocaine in the world. It has caused relations with other countries such as United States to be problematic (US department of state, 2014).

The country has been plagued by many revolutions and dictatorships in the 20th century (Mesa Gisbert et al, 2012). . Fortunately recent democratization have helped to improve the conditions, especially for the indigenous population. However the conditions are not sufficiently good in some areas e.g. access to water. In large cities like Cochabamba only some areas have constant access to drinking water and the water in parts of the Altiplano is contaminated with mining waste (Mehta et al, 2014, and Goix et al, 2011).

Figure 1: Location of Bolivia and Oruro (Google Inc, 2015)

The Altiplano

The Altiplano has an arid climate with rainfall mainly in the summer (Nationalencyklopedin, 2015). The summer rains can be very heavy causing problem with flooding in some areas, with the total amount of rainwater each year still being low, causing problems with water shortage (Ivarsson & Lindström, 2015).

The Altiplano has some of the highest altitude cities in the world such as La Paz, Oruro and Potosi, and the highest lake with boat traffic, Lake Titicaca (Nationalencyklopedin, 2015). All of them are situated more than 3500 m above sea mean level. The Altiplano is very rich in natural resources, e.g., natural gas and metals such as tin, silver, and the recently discovered lithium, which have given rise to mining cities such as Potosi and Oruro where mining has been practiced for 400 years (Benchwick & Smith, 2013). The wealth of the mining cities is dependent on the access to and market price metal ore, causing economic booms when the supply and price are high, and economic depressions when the metal has come to an end or the price is low (Benchwick & Smith, 2013). Economic depressions have been more common during later years causing problems with poverty (Benchwick & Smith, 2013).

The mining brings not only a source of income to the cities, but causes also severe problems. The working conditions in the mines are terrible and the mining waste contaminates both the soil and water with heavy metals (Goix, et al, 2011, and Ramos, et al, 2014). However the heavy metals also occurs naturally in the soil. The sum of both the anthropogenic and natural sources is levels of heavy metals that are higher than the guidelines of the European Union and the World Health Organization, respectively, meaning that the water is not safe to drink (Goix et al, 2011, and Ramos et al, 2014).

Oruro

Oruro is a mining city in the Altiplano with a population of about 300,000 people and located on an altitude of 3600 m above mean sea level. The climate of Oruro is arid with an average annual rainfall of 383 mm but with large variation between years, see *Figure 2* (Servicio Nacional de Meterología e Hidrología, Bolivia, 2015). Oruro has environmental problems typical for the area which are droughts, floods, and metal pollution (Nationalencyklopedin, 2015, and Ramos, et al, 2014). Some of these problems have been studied in detail in the doctoral thesis by Calizaya Terceros (2009) and bachelor thesis by Ivarsson & Lindström(2015). The main anthropogenic source of metal pollution is the San José mine which is located inside the city, contributing to metal contamination in the vicinity of the mine (Google, 2015, and Dames & Moore Norge and Comibol, 2000). Oruro gets the major part of its water from the Challapampa groundwater aquifer, which consists of thick layers of alluvial sediments surrounded by sedimentary bedrock.

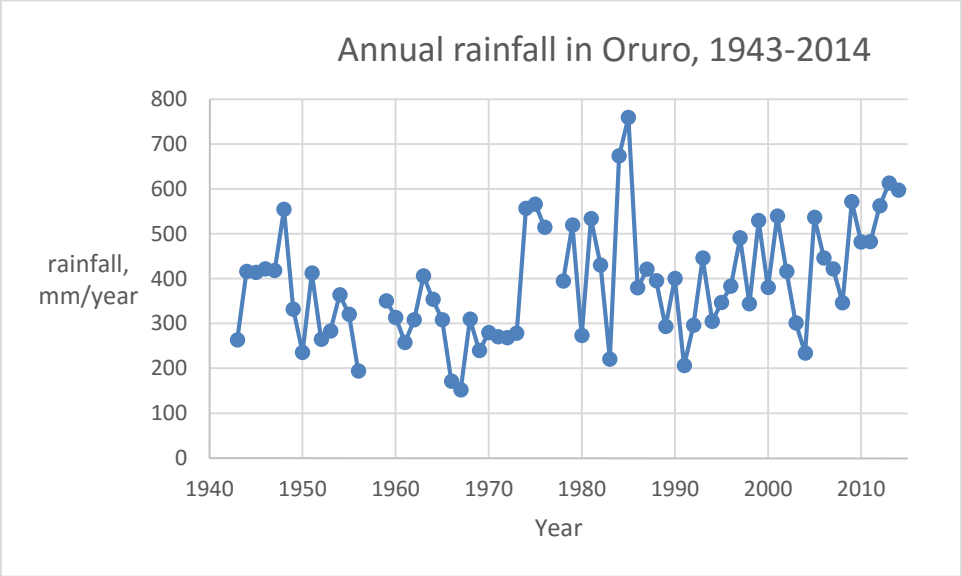

Figure 2: Annual rainfall in Oruro 1943-2013 (Servicio Nacional de Meterología e Hidrología, Bolivia, 2015)

Challapampa aquifer

The Challapampa is a large groundwater aquifer situated north of Oruro, see Figure 3. The aquifer is divided in two parts with the alluvial fan shown in Figure 3 and 4 being the most important part for groundwater extraction. The area is subject for the research by PhD students Claudia Canedo and Etzar Gomez. The recharge of the aquifer occurs mainly from the Paria River, see Figure 3, just north of the aquifer, and the area overlaying the aquifer (Canedo, 2014).

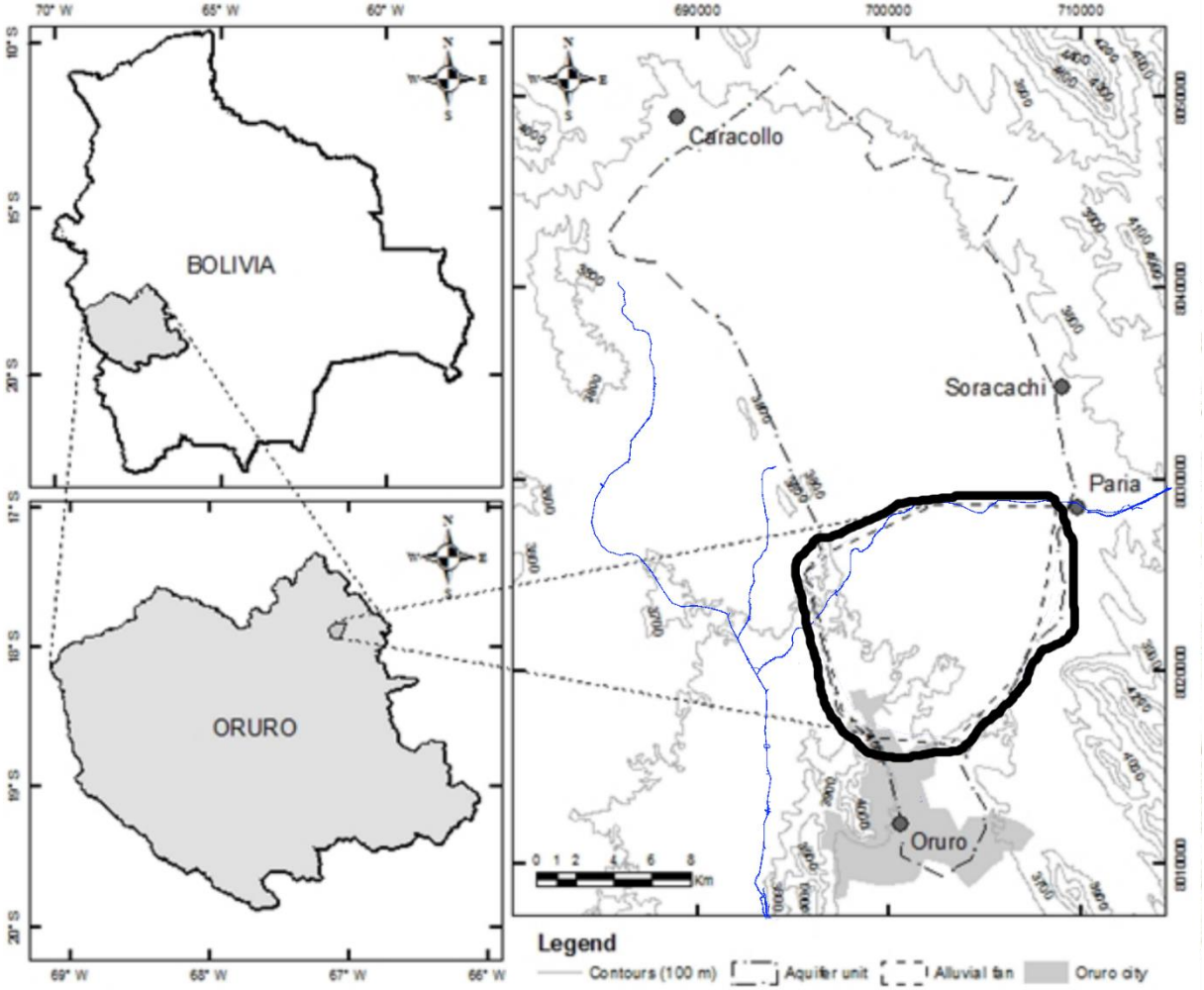

Figure 3: Thick black line marks the alluvial fan which is the research area for PhD students Etzar Gomez and Claudia Canedo. The dashed line marks the whole aquifer and the blue line marks the major rivers in the area (Gomez, 2014; ArcGIS, 2014)

Large areas of the aquifer are unmapped regarding hydrogeological properties as the designation "alluvial deposits" covers a range of soil types, see Figure 4. PhD student Etzar Gomez mentions that studies have been performed in the area, but the exact location of the measurements is unknown or unclear and therefore they remain largely unusable. Furthermore some of the studies have not been made available to the public. Altogether, it means that investigations are repeated despite that the information already exists.

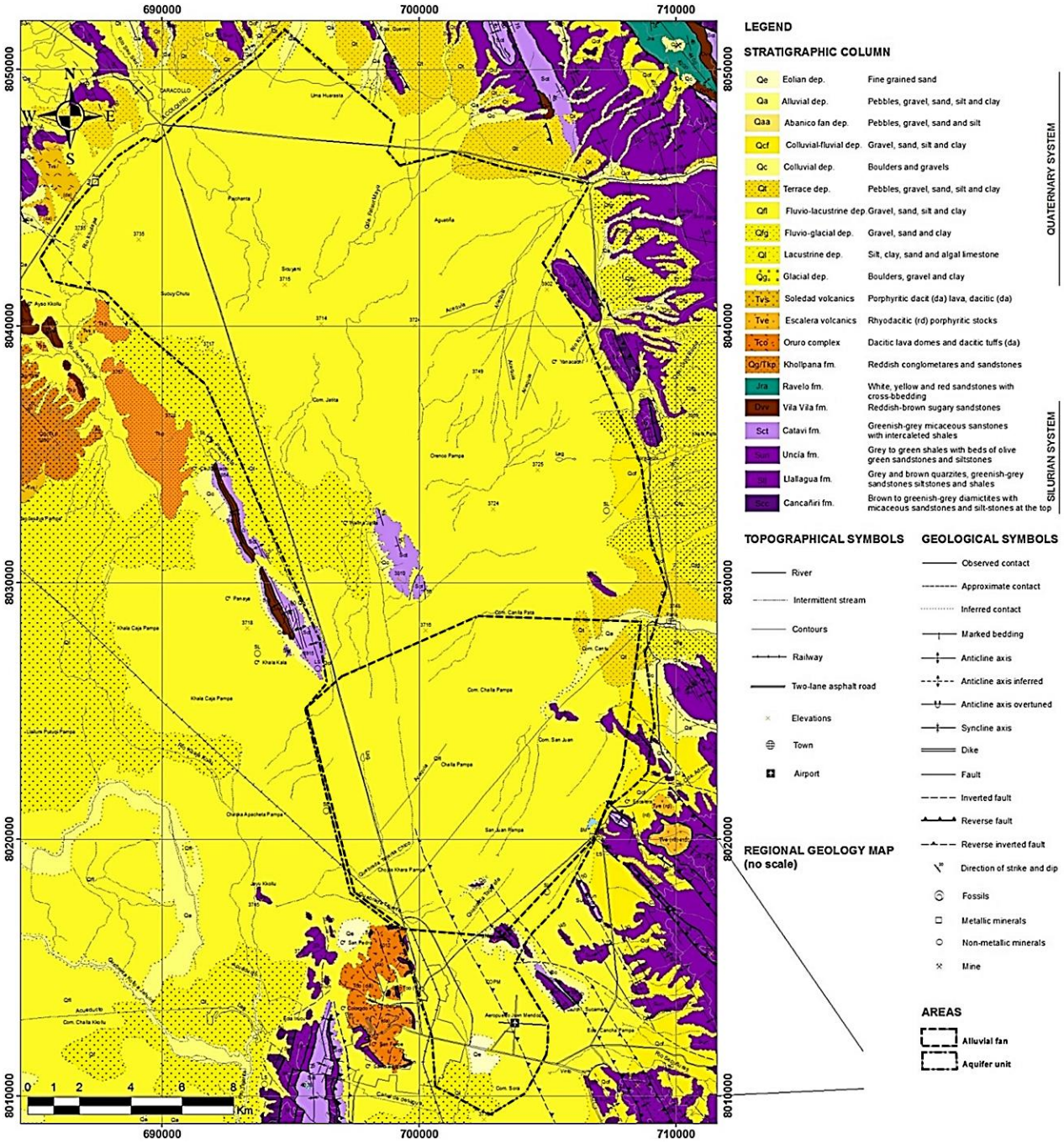

Figure 4: Geological map of the study area (GEOBOL & Swedish Geological AB, 1992)

The risk of metal polution was studied by Canaviri Blanco(2011) who showed that most of the aquifer, 83%, do not have a high risk of metal contamination and that the areas with the highest risk are located near the San José mine. The aquifer also contains volcanic springs with highly saline water. The extension of the plume of volcanic water is largely unknown which may cause problems for future drillings for groundwater.

The aquifer consists of subunits divided by clay lenses that are assumed to be connected (Gomez, 2014). An example of the constitution of the aquifer at small scale is shown in Figure 5.

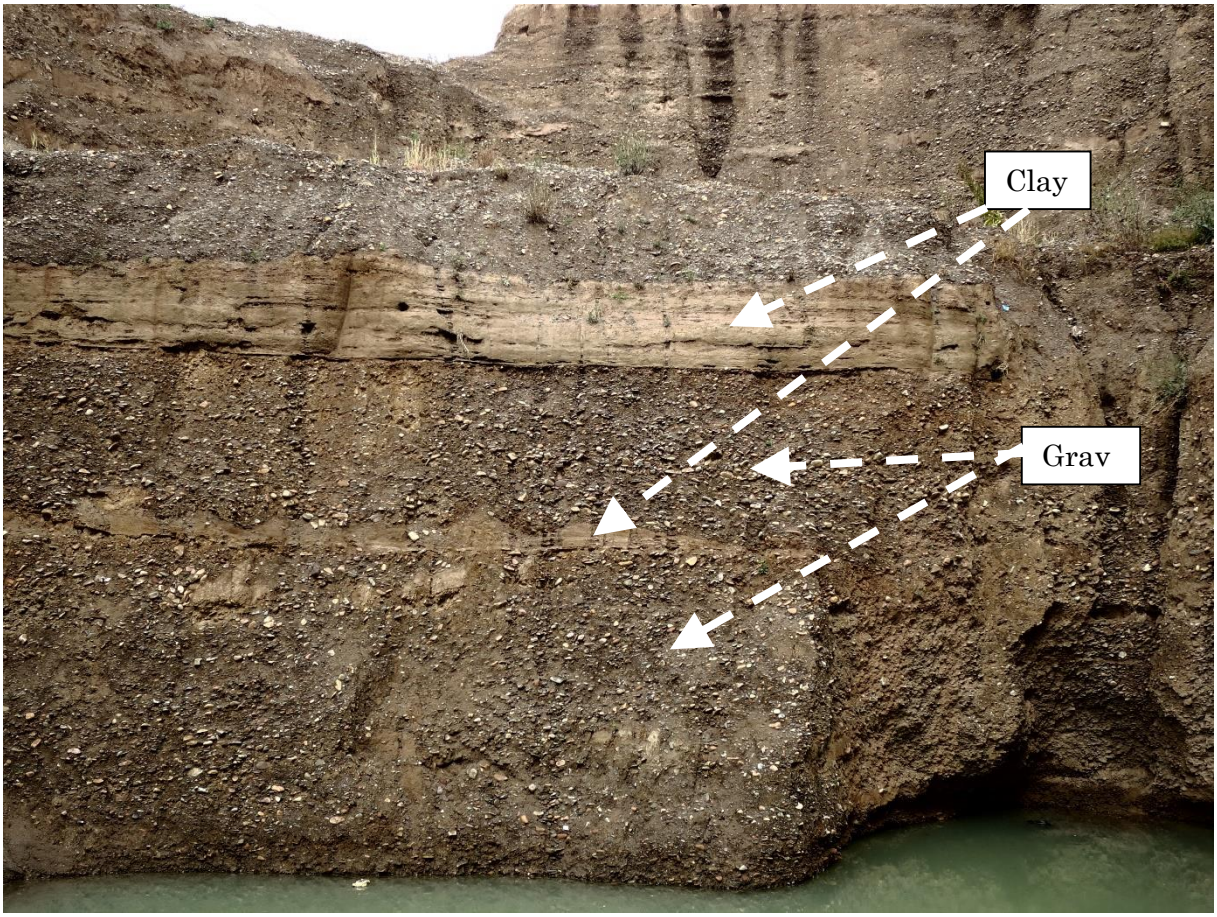

Figure 5: A small part of the aquifer, at coordinates UTM 19S 0703708 8029365, showing a typical distribution of different layers with different grain sizes, photo Martin Rosén

Study site

The study site is located in the village of Paria, adjacent to the Paria river, see Figure 6-8. The area is flat and comprised of fallow fields with some of the natural vegetation, consisting of grass and cacti, see Figure 8. The type of vegetation is typical for the Altiplano and thus present on other parts of the aquifer. The location was selected because of the possibility to store equipment, it is easy to access by public transportation and, as mentioned before, the vegetation is present on other parts of the aquifer.

Figure 6: Location of the village Paria close to the city Oruro (Google Inc, 2015).

Figure 7: The location of study site within the village Paria, broken line (Google Inc, 2015).

Figure 8: The study site indicated by the broken line. Photo: Martin Rosén

Methods and theory

Infiltration

Infiltration is the process of water entering soil and its subsequent movement through the soil (Brutsaert, 2005). The infiltration mainly occurs as flow through macropores which can be classified as pores larger than 75µm (Kirkham, 2005). The infiltration is affected a number of factors such as precipitation, base flow, soil characteristics, soil saturation, land cover, slope, evapotranspiration (US Geological Survey, 2015). In the study the infiltration was assumed to only be affected by soil saturation. The study area was very small and therefore other factors were assumed to be constant.

The hydraulic conductivities for a range of sediments are presented in table 1. These are for soil without tension, i.e. h=0

Table 1: Hydraulic conductivity for unconsolidaded sediments (Fetter, 2001)

Material	Hydraulic conductivity (m/s)
Clay	10^{-11}-10^{-8}
Silt, sandy silt, clayey sand	10^{-8}-10^{-6}
Silty sand, fine sand	10^{-7}-10^{-5}
Well sorted sand, glacial outwash	10^{-5}-10^{-3}
Well-sorted gravel	10^{-4}-10^{-2}

Horton's equation

In 1930 Robert E. Horton noted that the infiltration was rapid in the beginning and after some time it approached a constant value. His work resulted in the Horton equation (Kirkham, 2005):

$$i = i_f + (i_0 - i_f) * e^{-\beta t}$$

EQ1

where

i_0 is the initial infiltration rate at t=0, in $\frac{mm}{min}$

i_f is the final constant infiltration rate in $\frac{mm}{min}$

ß is a soil parameter describing the rate of decrease of infiltration

The reason for the infiltration decreasing with time is, according to Horton, due to processes on the soil surface such as swelling of soil particles and sealing of small cracks (Kirkham, 2005). The constant infiltration rate i_f is analogous to the saturated hydraulic conductivity and is used by some methods with the tension disc infiltrometer, e.g. the method by Ankeny et al(1991).

Tension disc infiltrometer

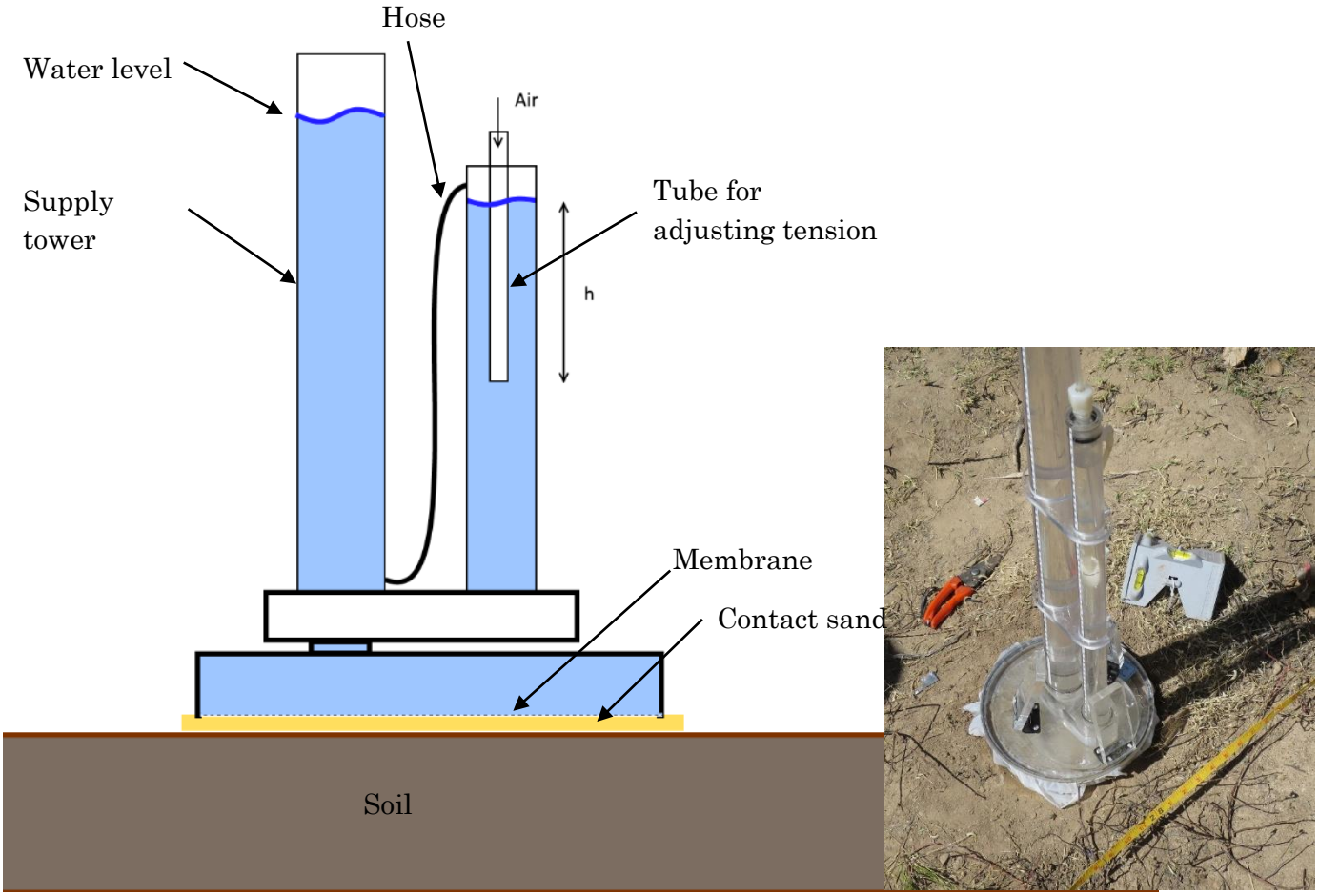

Figure 9: Schematic picture of a measurement with the tension infiltrometer

Description of instrument

The tension disc infiltrometer is a standard measuring device for estimating unsaturated hydraulic conductivity (Kirkham, 2005). It consists of two tubes connected with a hose, see Figure 9. The larger tube, the supply tower is connected to the soil via a disc with a membrane. The membrane is one of the major weaknesses of the instrument because it is easily damaged and difficult to replace (Soil Measurement Systems, 2015). To assure sufficient hydraulic connection, contact sand is required between the disc and the soil. The smaller tube is connected to the air via a smaller adjustable tube, which is used to set the tension.

The infiltrometer prevents water from entering large cracks and thus assures that only infiltration through the soil is measured. It is done by applying a small negative pressure, a tension, on the water while it enters the soil through a fine membrane (Soilmoisture equipment corp., 2008). The higher the tension the more soil pores are without water and thus the soil is less saturated (Soil Measurement Systems, 2005). The relationships between tensions and infiltration rates are used to determine the hydraulic conductivity. Normally two tensions are used (Soilmoisture equipment corp., 2008).

Measurement procedure

Here follows a description example of a measurement, essential for understanding the results. Two measurement with different tensions were used: K1 for hydraulic conductivity at tension 1 and K2 for hydraulic conductivity at tension 2

1. It is crucial that the measurement is performed on a leveled surface and because the measurement spot needs to be checked with a level even before preparation of the surface.
2. The soil surface is cleaned from debris and occurring plant stems and/or grass are removed. However, it is important that the soil surface itself is not disturbed.
3. The guide ring is placed on the spot and the contact sand is added until a completely flat and leveled surface is achieved, see Figure 10. The contact sand was taken from the nearby river bank.

Figure 10: The soil is prepared for measurement

4. The tension is set with the adjustable tube, see Figure 9. The clamp around the hose should be closed.
5. The supply tower is filled with water. It is easily done by placing the instrument in a bucket with water and suck water into the instrument via the small hose on top of the supply tower, see Figure 11.

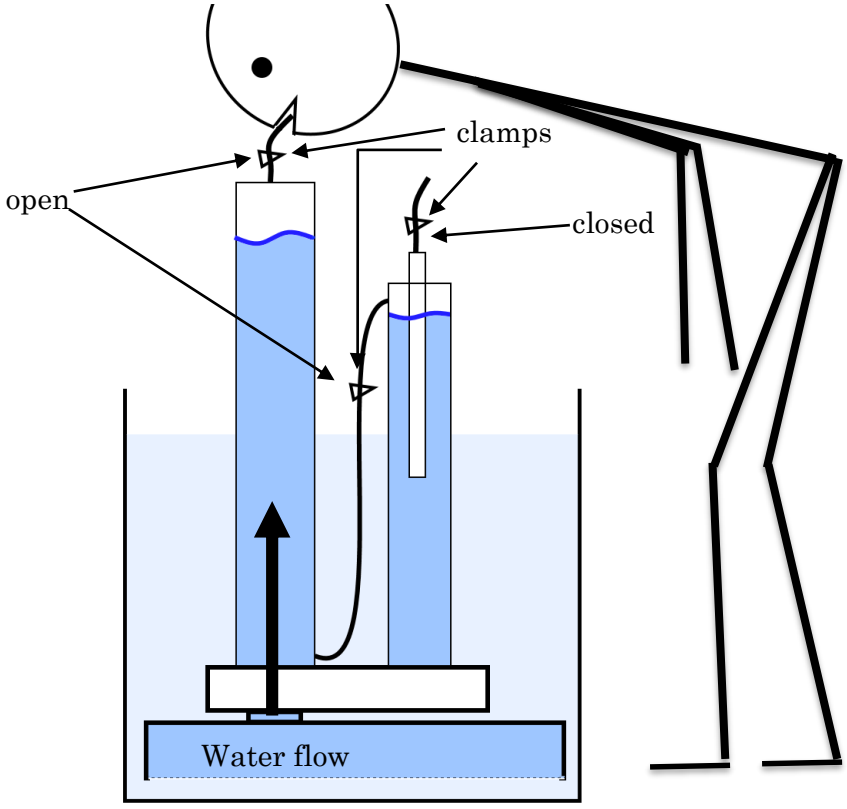

Figure 11: Filling the instrument with water by sucking water through the supply tower

6. All the clamps are closed before placing the instrument on the prepared surface.
7. The instrument is placed on the prepared surface, water level in the supply tower is noted.
8. The measurement is started by opening the clamp on the tension tower and the clamp on the hose.
9. The water level in the supply tower is recorded every two minutes until constant infiltration rate is reached, i.e. 4 consecutive measurements with the same change in water level.
10. To stop the measurement the clamp on the tension tower is closed and the instrument is removed from the measurement surface, most easily into the water bucket.
11. The procedure for steps 4-11 is repeated for the second measurement.

Method using constant infiltration rate

Method I

The method described in the infiltrometer manual rely on the constant infiltration rate described in EQ1 (Soilmoisture equipment corp., 2008). The method is based on Wooding (1968) and was developed by Ankeny et al(1991). A disadvantage of the method is that constant infiltration rate is difficult to reach, within normal measurement times of one hour, if the hydraulic conductivity in the soil is low (Zhang, 1998).

It uses an algebraic approximation for flow from a circular source (Wooding, 1968):

$$Q = \pi r^2 K\left(1 + \frac{4}{\pi r \alpha}\right)$$

EQ2

where

Q is the volume of water entering the soil per unit time, at constant infiltration rate, in $m^3 s^{-1}$

K is the hydraulic conductivity in $mm*min^{-1}$

α is a constant

r is the radius of the source, i.e., the infiltrometer

K is assumed to vary with the matrix potential of the water source (Gardner, 1958). It results in:

$$K(h) = K_{sat} * e^{\alpha h}$$

EQ3

where

K_{sat} is the saturated hydraulic conductivity

h is the matrix potential, or tension, in cm

Combining EQ2 and EQ3 gives:

$$Q = \pi r^2 K_{sat} * e^{\alpha h}\left(1 + \frac{4}{\pi r \alpha}\right)$$

EQ4

To calculate the hydraulic conductivity at least two measurements with different tensions are required, giving:

$$Q(h_1) = \pi r^2 K_{sat} * e^{\alpha h1}\left(1 + \frac{4}{\pi r \alpha}\right)$$

EQ5

and

$$Q(h_2) = \pi r^2 K_{sat} * e^{\alpha h2}\left(1 + \frac{4}{\pi r \alpha}\right)$$

EQ6

Combining EQ6 and EQ7, and solving for α, gives:

$$\alpha = \ln\left(\frac{Q(h_2)}{Q(h_1)}\right) * \frac{1}{h_2 - h_1}$$

EQ7

When α is calculated, K_{sat} is calculated from EQ5 or EQ6. K_{sat} is then inserted into EQ3 to get the hydraulic conductivity at any tension. When comparing the results from the tension infiltrometer with results from double ring infiltrometers, the values obtained for K_{sat} might differ. The reasons are that K(h) might not be linear near h=0 and that the tension infiltrometer restricts the flow so that water will not enter the very large pores and cracks. It is not the case for the double ring infiltrometer, another commonly used measurement instrument. When α is calculated, the hydraulic conductivities for the different tensions can be calculated from EQ3.

$$K1I = K_{sat} * e^{\alpha*(-0.1)}$$

EQ8

$$K2I = K_{sat} * e^{\alpha*(-0.05)}$$

EQ9

Methods using the cumulative infiltration equation

Because of the difficulties to reach constant infiltration rate used in Method 1, other methods have been developed such as techniques by Zhang(1998), Warrick(1992), and Haverkamp et al. (1994). They rely on the cumulative infiltration equation (Angulo-Jaramillo et al, 2000):

$$I = C_1 t^{1/2} + C_2 t$$

EQ10

Where

C_1 describes the infiltration in its early stage

C_2 is the constant infiltration rate

The difference between the methods concerns the constants C_1 and C_2. Zhang(1998) assumes that they are dependent on the hydraulic conductivity whereas Haverkamp et al(1994) and Warrick (1992) assume that the constants are dependent of the sorptivity and hydraulic conductivity.

EQ10 is affected by the layer of contact sand, which influences the infiltration at its early stage where these methods have their applicability (Haverkamp et al., 1994). The contact sand layer affects the measurement by causing a rapid infiltration in the beginning of the infiltration experiment. It causes inaccurate estimations of the parameters C_1 and C_2 in EQ10. The constants C_1 and C_2 are also affected by the intercompensation of $t^{1/2}$ and t (Vandervaere et al, 2000). If the effect results in that C_2, constant infiltration rate, becomes less than zero it means that the two-parameter equation does not have physical meaning (Vandervaere et al, 2000).

Differential linearization

One way to detect the effect of the contact sand is to use differentiated linearization, where the changes in infiltration rate become more apparent (Vandervaere et al, 2000). The differentiated linearization is a method developed to detect and account for the effect of the contact sand (Vandervaere et al, 2000). It executed on EQ10 with the infiltration, I, being differentiated with $\sqrt{t}$ (Vandervaere et al, 2000):

$$\frac{dI}{d\sqrt{t}} = C_1 + 2C_2\sqrt{t}$$

EQ11

where the derivative is approximated by the change in infiltration by square root of time:

$$\frac{dI}{d\sqrt{t}} \approx \frac{\Delta I}{\Delta\sqrt{t}}$$

and

$$\sqrt{t}$$

is calculated as the geometric mean:

$$\sqrt{t} = \left(\sqrt{t_i * t_{i+1}}\right)^{1/2}$$

EQ12

If $\frac{dI}{d\sqrt{t}}$ is plotted against $\sqrt{t}$, and a line is fitted to the data, the constant C_1 correspond to the value where the line intersects the y axis and C_2 will be half the slope, see EQ11 and Figure 12. C_1 and C_2 can then be used to calculate the hydraulic conductivity. The differentiation makes changes in slope very apparent, see Figure 12. It makes it possible to detect the effect of the contact sand and removing it by omitting the first readings. Once the effect is detected, the same readings can also be removed from a curve fitting using cumulative infiltration.

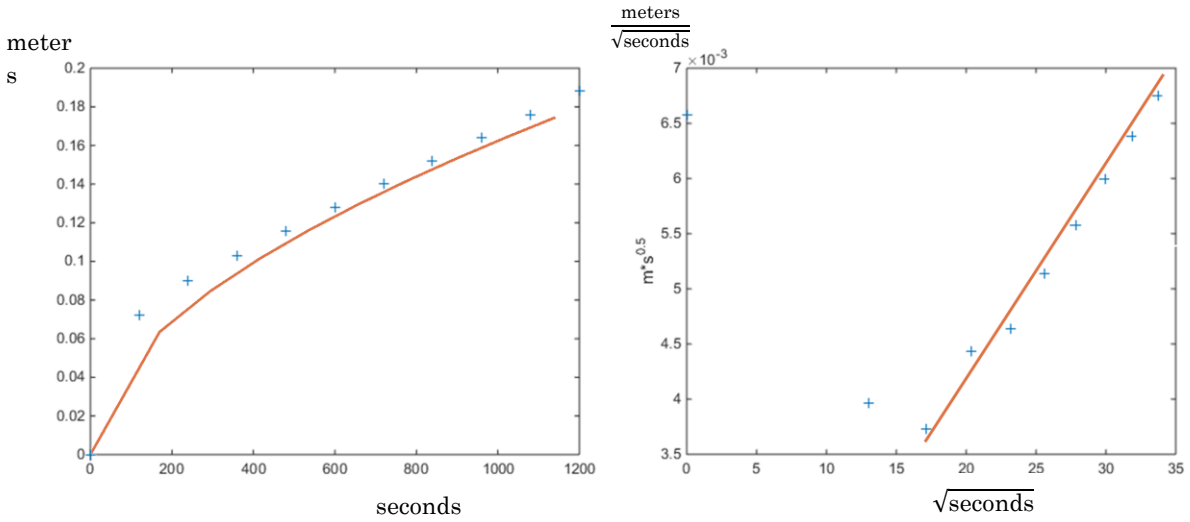

Figure 12: The left picture shows a curve fitting using cumulative infiltration. The right picture shows curve fitting using differentiated linearization. Note the rapid changes in slope for the first three readings, in the right picture, which makes it possible to detect the effect of the contact sand. The effect is invisible in the left picture.

Method II

Zhang (1998) developed a method for calculating hydraulic conductivity with the tension infiltrometer. It is based on the cumulative infiltration equation, EQ10, described above. Taking the derivative of EQ10 yields a function of the infiltration rate over time:

$$\mathrm{i} = 0.5\mathrm{C}_1\mathrm{t}^{-1/2} + \mathrm{C}_2$$

EQ13

Assuming that the steady state infiltration rate $i_s = C_2$ we have:

$$i = 0.5C_1t^{-1/2} + i_s$$

EQ14

The correction factor $\mathrm{f}=\frac{\mathrm{i}}{\mathrm{i_s}}=\frac{\mathrm{Q}}{\mathrm{Q_s}}$ becomes:

$$\mathrm{f} = \frac{0.5\mathrm{C}_1\mathrm{t}^{-\frac{1}{2}} + \mathrm{C}_2}{\mathrm{C}_2}$$

$$\mathrm{f} = 0.5\frac{\mathrm{C}_1}{\mathrm{C}_2}\mathrm{t}^{-\frac{1}{2}} + 1$$

EQ15

For two different supply pressures the correction factors becomes:

$$\mathrm{f}_1 = 0.5\frac{\mathrm{C}_{1,1}}{\mathrm{C}_{1,2}}\mathrm{t}_1^{-1/2} + 1$$

EQ16

and

$$\mathrm{f}_2 = 0.5\frac{\mathrm{C}_{2,1}}{\mathrm{C}_{2,2}}\mathrm{t}_2^{-1/2} + 1$$

EQ17

To find $\mathrm{C}_{1,1}$, $\mathrm{C}_{1,2}$, $\mathrm{C}_{2,1}$ and $\mathrm{C}_{2,2}$ curve fitting of the infiltration data to EQ10 is required. Then the macroscopic capillary length can be determined as:

$$\lambda = \frac{\Delta\mathrm{h}(\mathrm{Q}_1\mathrm{f}_2 + \mathrm{Q}_2\mathrm{f}_1)}{2(\mathrm{Q}_1\mathrm{f}_2 - \mathrm{Q}_2\mathrm{f}_1)}$$

EQ18

The hydraulic conductivities can then be determined as:

$$K1II = \frac{\frac{Q_1}{f_1}}{\pi r_d^2 + 4\lambda r_d}$$

EQ19

$$K2II = \frac{\frac{Q_2}{f_2}}{\pi r_d^2 + 4\lambda r_d}$$

EQ20

Were r_d is the radius of the infiltrometer disc

For soils with sufficiently high hydraulic conductivity Zhang (1998) showed that his method and the Ankeny et al. (1991) method does not have a significant difference.

Method III

Method III uses the differentiated linearization to get the constants C_1 and C_2 in EQ10 and then uses the technique of Zhang (1998) to calculate the hydraulic conductivities.

Measurement setup

To achieve a comparison of the different soil properties, a similar measurement setup as Selim et al (2011) was used, see Figure 13. The measurements covering the diagonals and the points in the center cover every 5 meters and the sparser points every ten meters. The grass shown in Figure 8 covers part of the northwest pointing diagonal, some measurements in the center and some in the northeast quadrant.

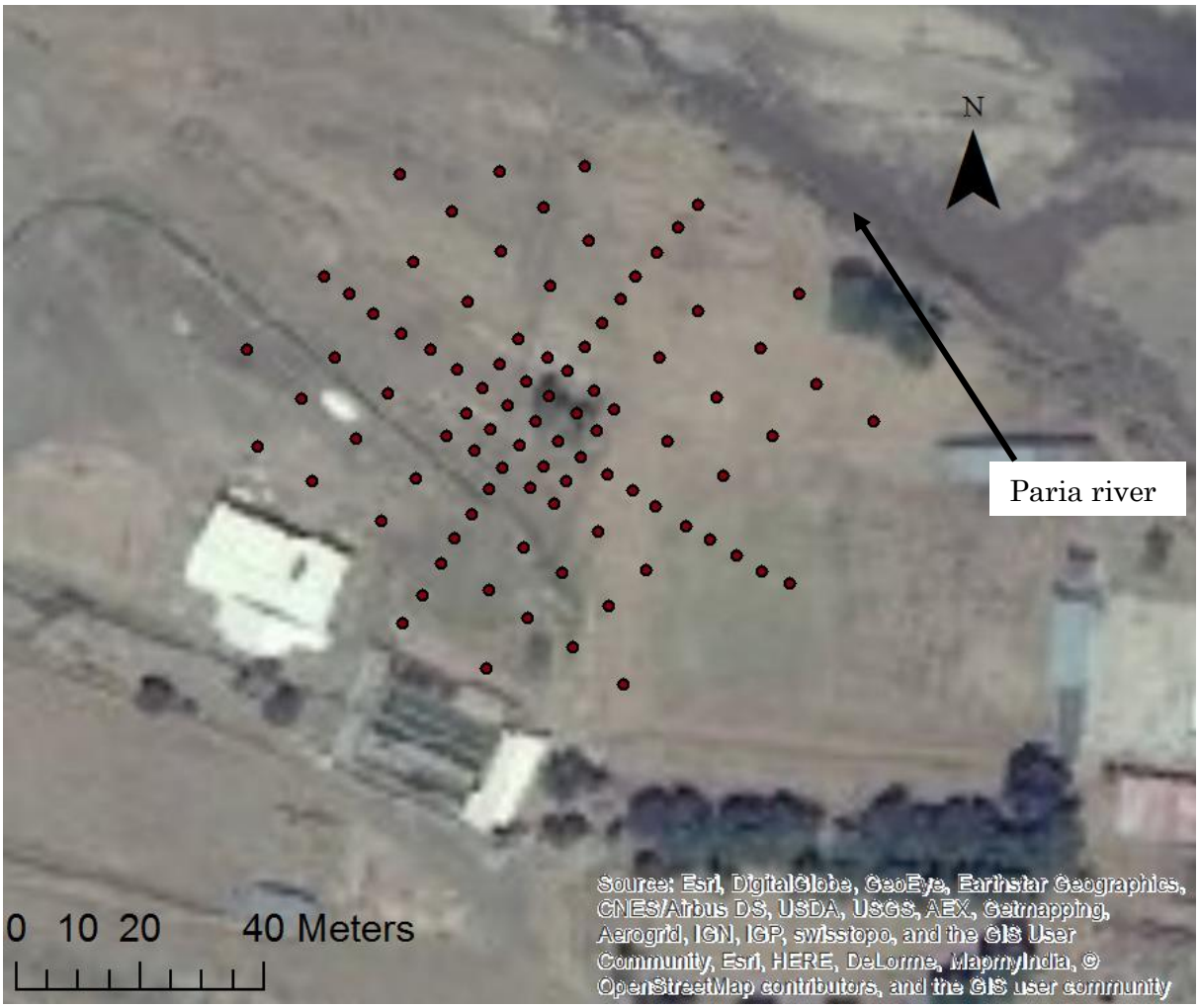

Figure 13: Experimental setup, similar to Selim et al (2011). The Paria river is the same as seen in the background of Figure 8

Interpolation

Several different interpolation methods were tested, with the spline being recommended by Denis Duda Costa at the Department of Water Resources Engineering at Lund University.

Spline

The interpolation method fits the relationship between the measurement points to a polynomial (ESRI, 2012). However, the polynomial creates two significant disadvantages: the interpolation near the borders may go on either direction, creating very low or high values in the borders. Also if two points are close to zero, the interpolation values in between them might be less than zero due to the curvature of the polynomial. In an attempt to mitigate the issue, virtual measurement points with the mean values, see Table 3, were added outside the experiment area.

Kriging

Kriging is a geostatistical interpolation method that, compared with other methods such as Inverse Distance Weighting (IDW), gives not only results, but also shows the accuracy of the interpolation results (Esri, 2014). Kriging applies the geographical principle that locations close to each other are more alike than locations far apart. The principle can be used to create a semivariogram to describe the relationship. A curve can then be fitted to the semivariogram. Depending on the spatial relationship, meaning the shape of the semivariogram, several different curves can be used e.g. spherical, Gaussian or linear. The curve is used to calculate the interpolation values. With the method, the difference of the measured value from the calculated value can be found and used in statistics to show the accuracy of the interpolation results.

Soil samples

The soil samples for point 1-36 were performed using a hoe. For the subsequent samples it was possible to use a soil sampler and thus soil samples for points 37-91 were collected using a soil sampler.

One soil sample at each depth, from 0-10 cm and from 10-20 cm, before and after the experiment were taken creating a total of four soil samples for each experiment. The samples were weighed before and after drying in oven at 105 degrees Celsius for 24 hours in metal containers (Department of Sustainable Natural Resources, 1990).Each of the 36 soil containers were weighted and marked before starting to measure the soil moisture content. The water content as a percentage was calculated according to:

$$\text{moisture content in \%} = 100 * \frac{(m_{before} - m_{after})}{m_{before}}$$

Results

Hydraulic conductivity

The hydraulic conductivity was measured at tensions h=-50mm and h=-100mm. The hydraulic conductivity at tension h=0 was also easily calculated with Method I. The three different methods described were used to calculate the infiltration values for all points. The effect of the contact sand was removed to as large extent as possible using differentiated linearization.

Many measurements resulted in negative values and these were discarded. However because the results were calculated during the field work it was possible to remake some of the measurements. That is the reason why the total amount of measurements is larger than the amount of measurement points. Also the very high result of point 42, K1I and K1III$\approx 3*10^{-1} ms^{-1}$, was discarded. The total amount of values discarded is shown in table 2.

Table 2: Number of results removed because of negative results.

Type	total amount of experiments	total amount discarded	in %
K1I	105	23	22
K2I	105	23	22
K0I	105	23	22
K1II	105	38	36
K2II	105	38	36
K1III	105	40	38
K2III	105	40	38

Summary of measurement values

The results of the hydraulic conductivity measurements is shown in Figure 14-16. The blue circles show hydraulic conductivity at tension h=-50mm and the brown squares shows hydraulic conductivity at tension h=-100mm. Only the positive results are shown, for all results see appendix. Figure 14 shows the results using Method I, Figure 15 shows the results using Method II and Figure 16 shows the results using Method III. The hydraulic conductivities have a range of 10^{-7}-10^{-5} m/s.

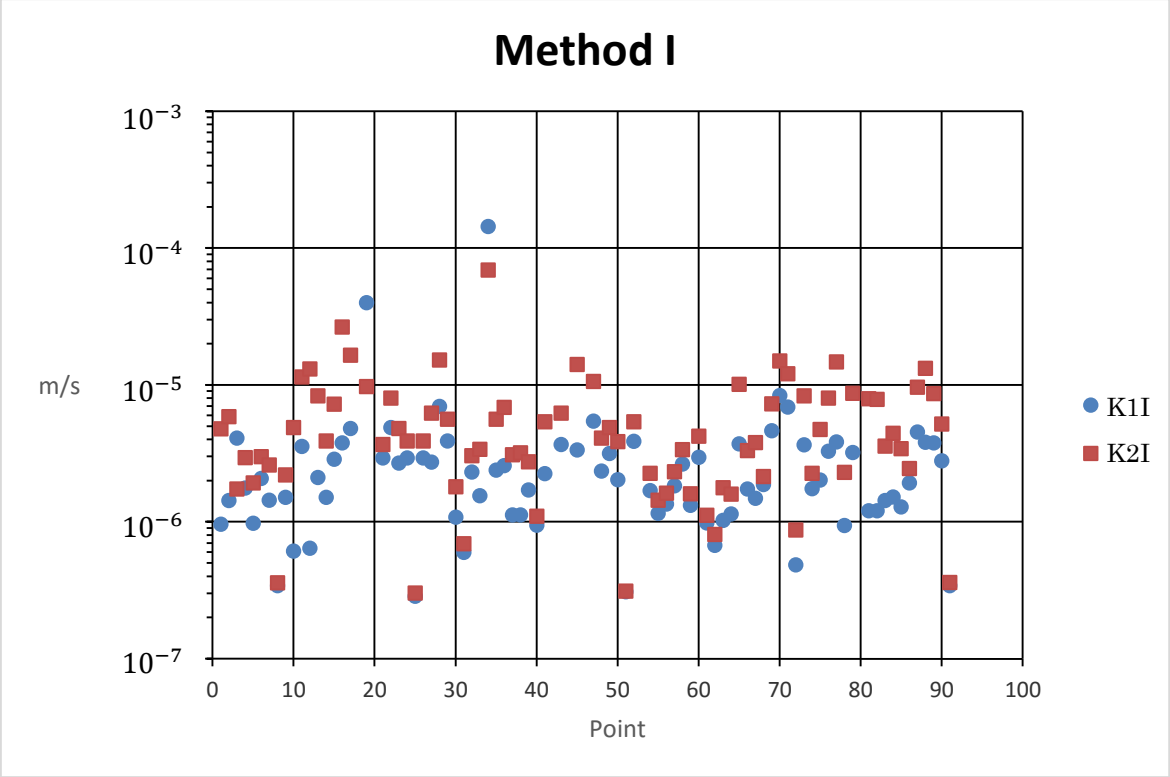

Figure 14: Summary of results regarding infiltration measured as vertical hydraulic conductivity for Method I

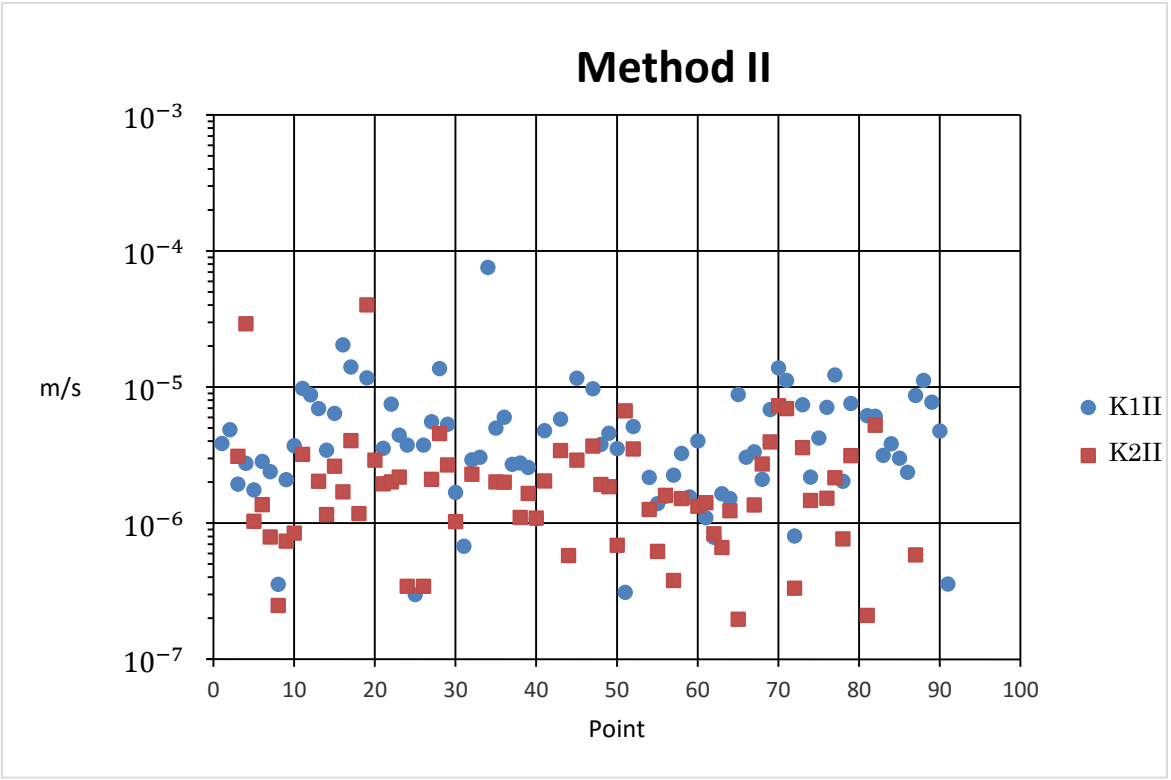

Figure 15: Summary of results regarding infiltration measured as vertical hydraulic conductivity for Method II

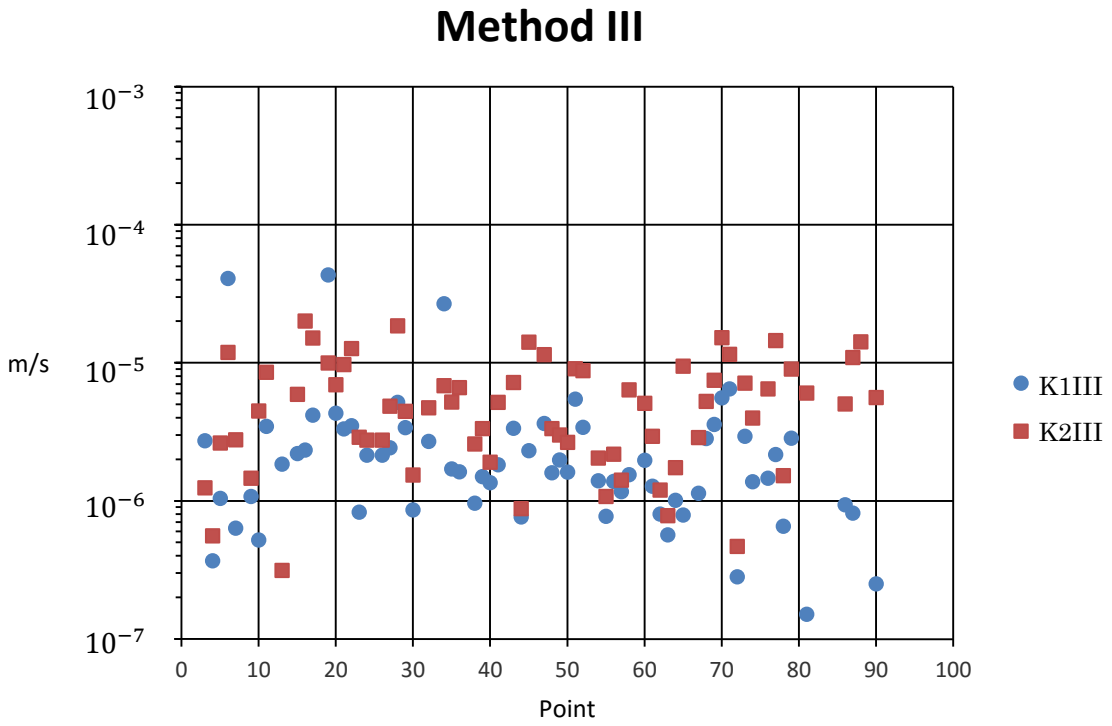

Figure 16: Summary of results regarding infiltration measured as vertical hydraulic conductivity for Method III

Descriptive statistics

The mean values and standard deviations for the hydraulic conductivities are shown in Table 3. Included are also the mean and standard deviation for tension h=0

Table 3: Mean values and standard deviations for in hydraulic conductivity using the different methods

Type	mean value(m/s)	Standard deviation (m/s)
K1I	$2.8*10^{-6}$	$4.4* 10^{-6}$
K2I	$5.5*10^{-6}$	$4.6*10^{-6}$
K0I	$1.8*10^{-5}$	$3.7*10^{-5}$
K1II	$2.0*10^{-6}$	$1.6*10^{-6}$
K2II	$5.9*10^{-6}$	$5.0*10^{-6}$
K1III	$2.0*10^{-6}$	$1.4*10^{-6}$
K2III	$5.8*10^{-6}$	$4.7*10^{-6}$

Probability distributions

To ensure statistic validity, the results were processed using Matlab to produce standard probability distribution plots. Because all the data seemed to fit the logarithmic normal distribution, only one example is presented here: hydraulic conductivity for K1I. For more plots see appendix

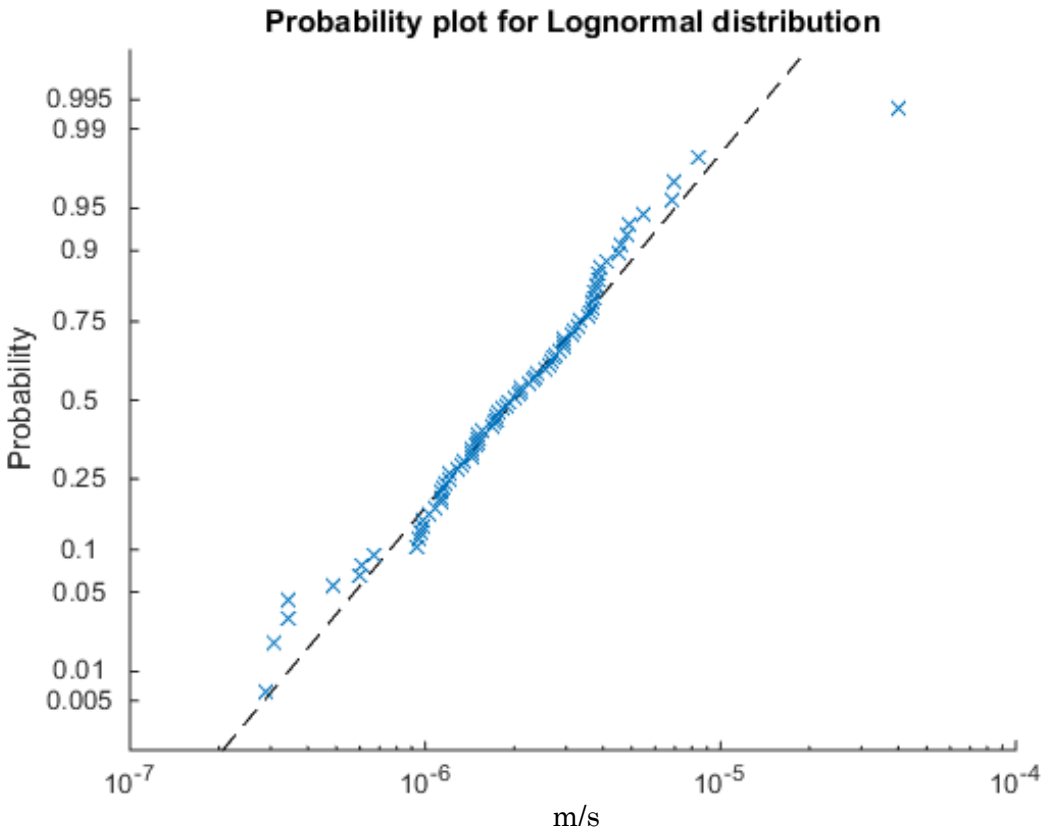

Figure 17: Probability distribution plot for logarithmic normal distribution, for K1I.

Interpolations

The interpolation results indicates the spatial variation of the hydraulic conductivities. In an effort to simplify comparisons, the color scheme have to a large extent been adjusted to show identical values across the diagrams.

Comparison between different interpolation results

Figure 18 shows a comparison between different interpolation methods and explains why the kriging interpolation method was selected for the spatial analysis. The data is from K1I. Some of the corners using the spline method are clearly higher and lower than the experiment results. Adding extra virtual points does not solve the problem completely. The kriging interpolation does not show the same tendencies. Similar results can be seen for K2I, see appendix.

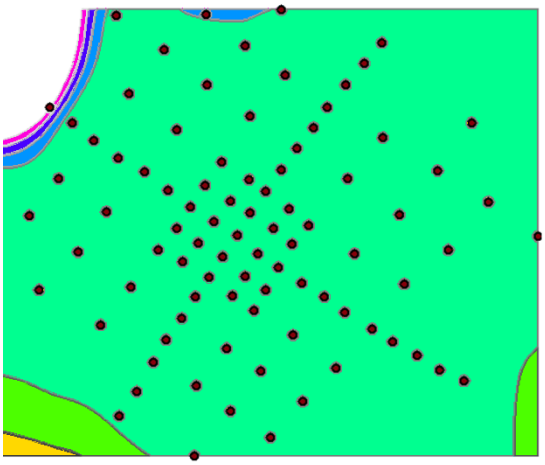

Soil moisture content at 10-20cm using spline

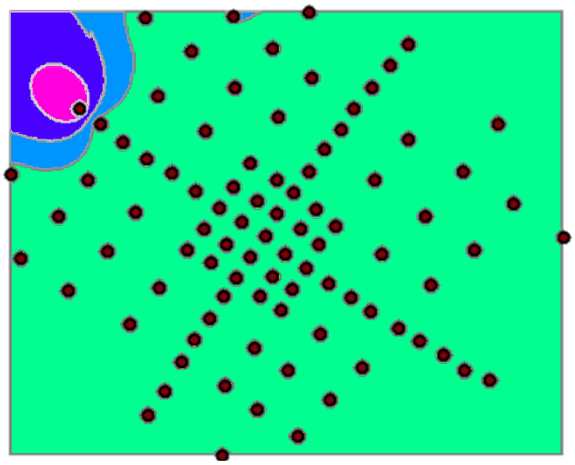

Soil moisture content at 10-20cm using kriging

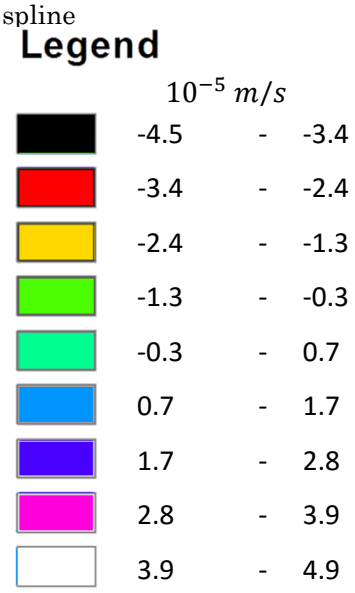

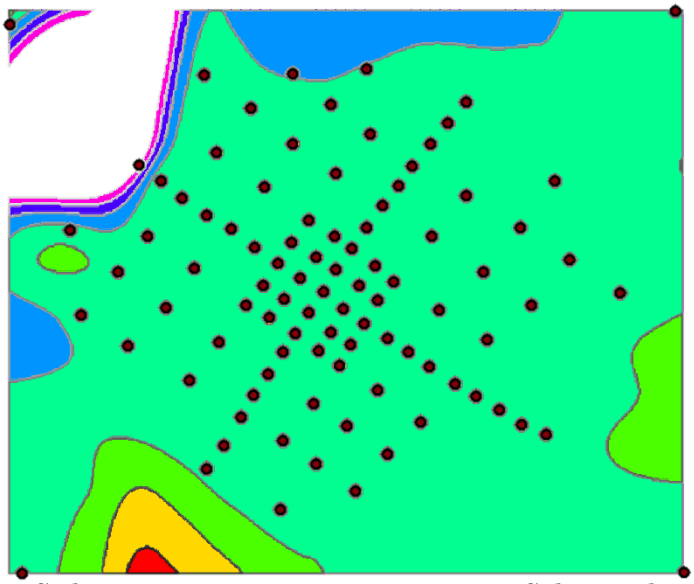

Soil moisture content at 10-20cm using Spline with virtual points

Figure 18: Hydraulic conductivity at K1I. with different interpolation methods. Shown are the problems with using the spline interpolation method; with very high or low values near the borders of the area. The problem is not fully re-solved when using virtual points outside the area. However kriging does not show these tendencies, even close to the point with high values of the hydraulic conductivity. The study area is shown in Figure 13

Interpolation results Kriging

Figure 19-22 show the spatial variation of the hydraulic conductivities. Figure 19-20 shows the results using Method I with Figure 20 showing hydraulic conductivity at tension h=0. Figure 21 shows the results using Method II and Figure 22 shows the results using Method III. There are clear patterns in the results but they do not seem to correlate between different methods.

Method I

Presented in Figure 19 are the results using Method I. Values for point 1 and 2 were recalculated using EQ3. The hydraulic conductivity for tension h=-100mm is larger in the west part with most of the results being above $2*10^{-6}$m/s. The hydraulic conductivity for tension h=-50mm show a clearer pattern with the east part and north part of the center being lower than other parts.

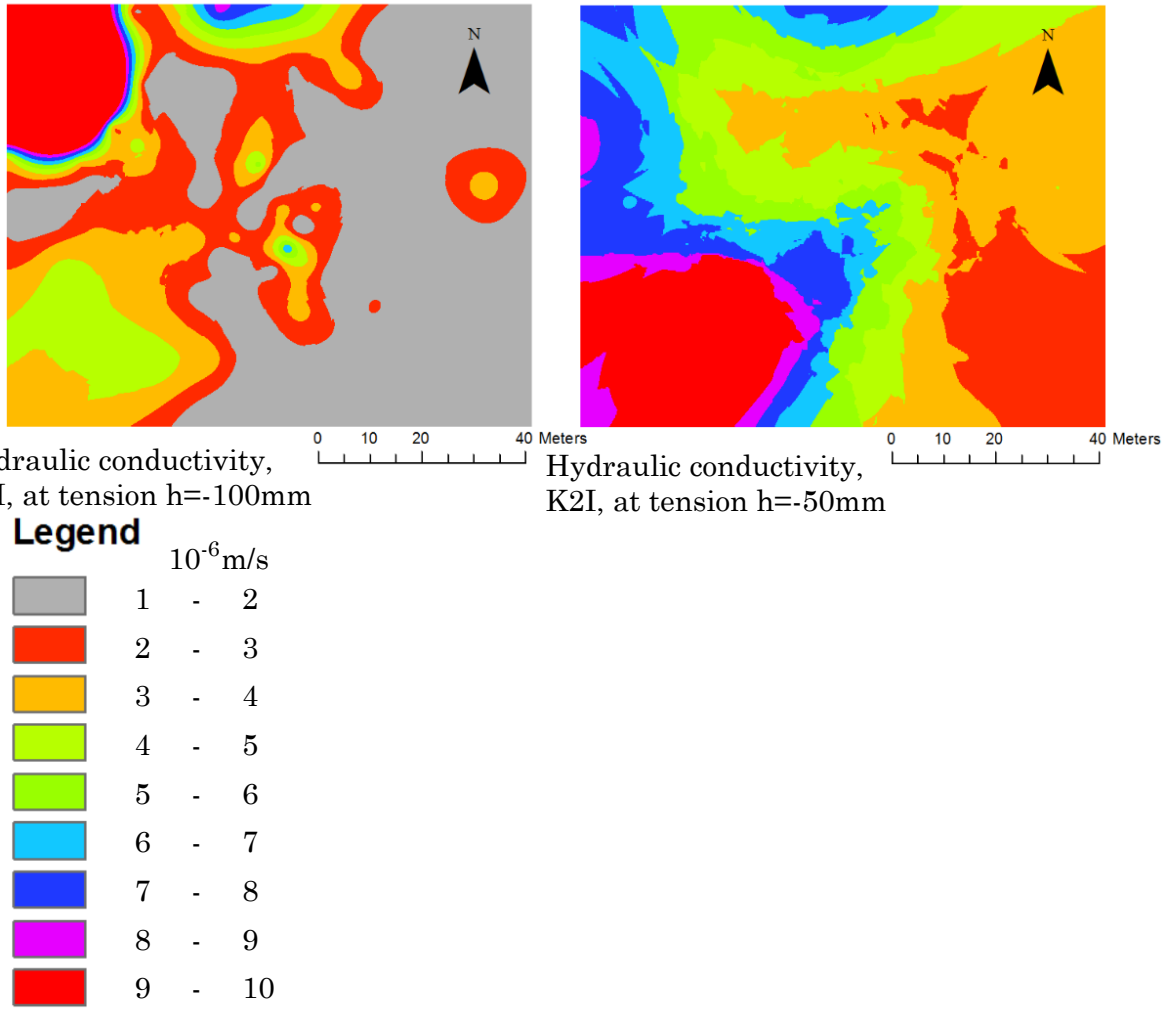

Hydraulic conductivity, K1I, at tension h=-100mm

Hydraulic conductivity, K2I, at tension h=-50mm

Figure 19: Hydraulic conductivity for K1I and K2I. The study area is shown in Figure 13

The hydraulic conductivity at tension h=0, shown in Figure 20, provides improved comparison between the reference values for soil. The pattern is similar to the hydraulic conductivity at tension h=50mm, see Figure 19, with the east part and north part of the center being lower than other parts

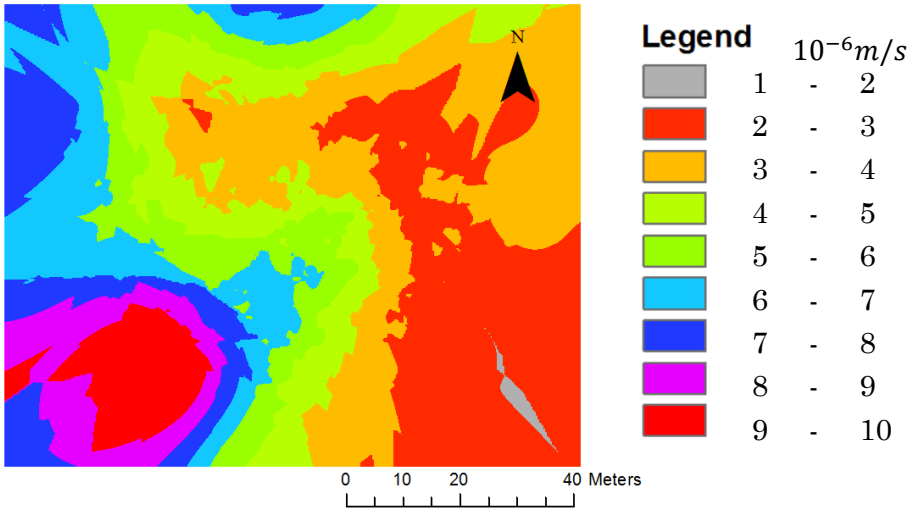

Figure 20: Hydraulic conductivity for K0I

Method II

Presented in Figure 21 are the results using Method II. The hydraulic conductivity for tension h=-100mm is larger in the northwest and central north part with most of the results being above $3*10^{-6}$m/s. The central part does also have somewhat larger conductivities than the rest. The hydraulic conductivity for tension h=-50mm is larger in the west part, above $6*10^{-6}$m/s. A smaller spot in the center also show larger conductivity than $6*10^{-6}$m/s. The east part have lower conductivities, less than $6*10^{-6}$m/s, with an area in the center also being lower than $6*10^{-6}$m/s

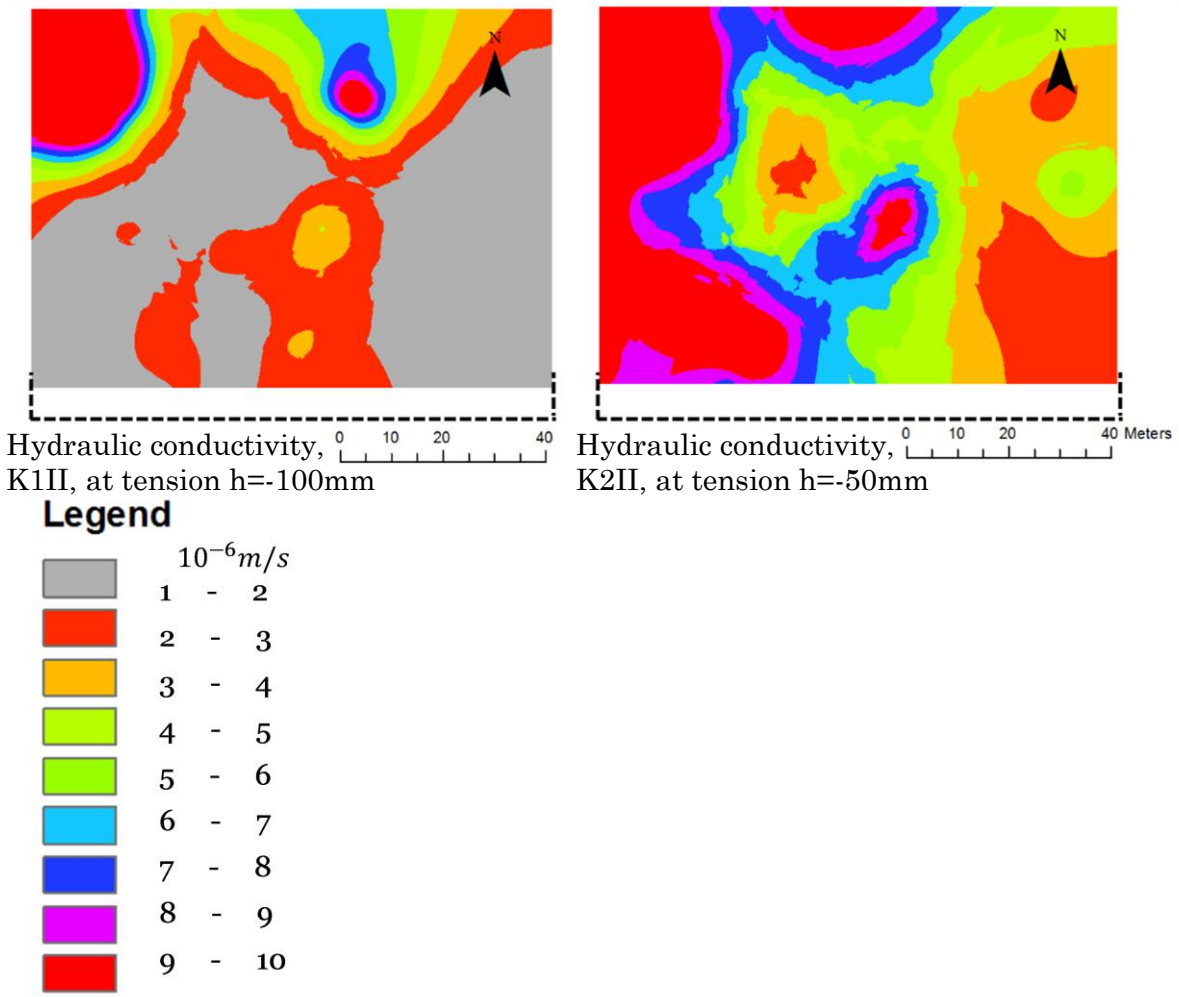

Figure 21: Hydraulic conductivity for Method II. The dotted line shows the extent of the study area that was not part of the interpolation because some results were discarded.

Method III

Presented in Figure 22 are the results using Method III. The hydraulic conductivity for tension h=-100mm is larger in the northwest and central part with most of the results being above $4*10^{-6}$m/s. The southwest and southeast part have lower conductivities. The hydraulic conductivity for tension h=-50mm is larger in the west part, above $6*10^{-6}$m/s. A smaller spot in the center also show larger conductivity than $6*10^{-6}$m/s. The east part have lower conductivities, less than $6*10^{-6}$m/s, with an area in the center also being lower than $6*10^{-6}$m/s

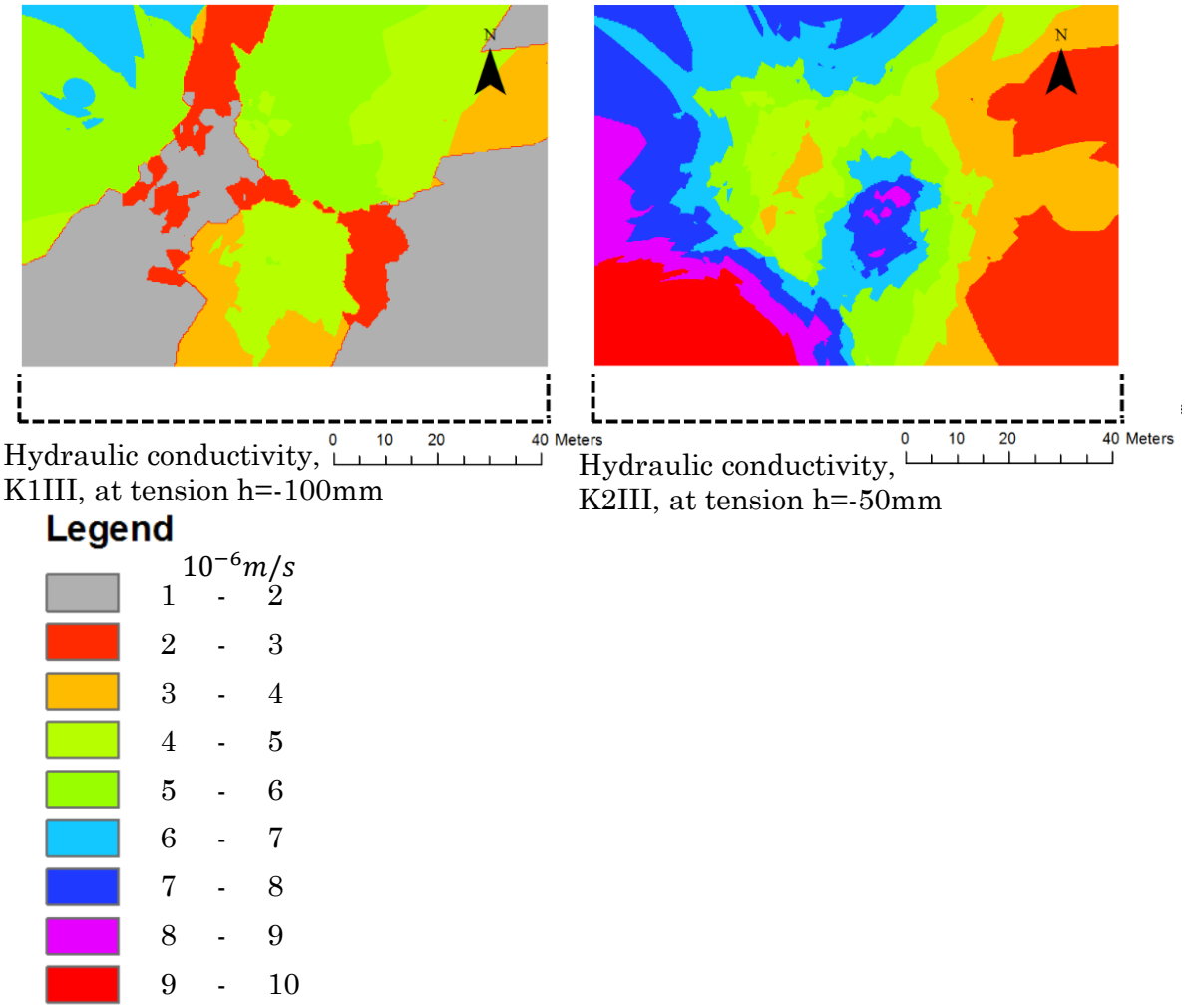

Figure 22: Hydraulic conductivity, K1III and K2III. The dotted line shows the extent of the study area that was not part of the interpolation because some results were discarded

Soil moisture content

The analysis of the soil moisture content was performed by university personnel at University Major de San Andres in La Paz. In total 440 soil samples were taken. Some replica soil samples were taken, with the mean being used in the analysis. The total amount of values and the amount of values discarded are shown in table 4

Table 4: Number of results replicated soil samples.

type	total amount	total amount discarded	in percent
0-10 cm	113	24	21
10-20 cm	108	23	21
0-10 cm after experiment	104	19	18
10-20 cm after experiment	105	19	18

Summary of measurement values

The results for each point are shown in Figure 23-24

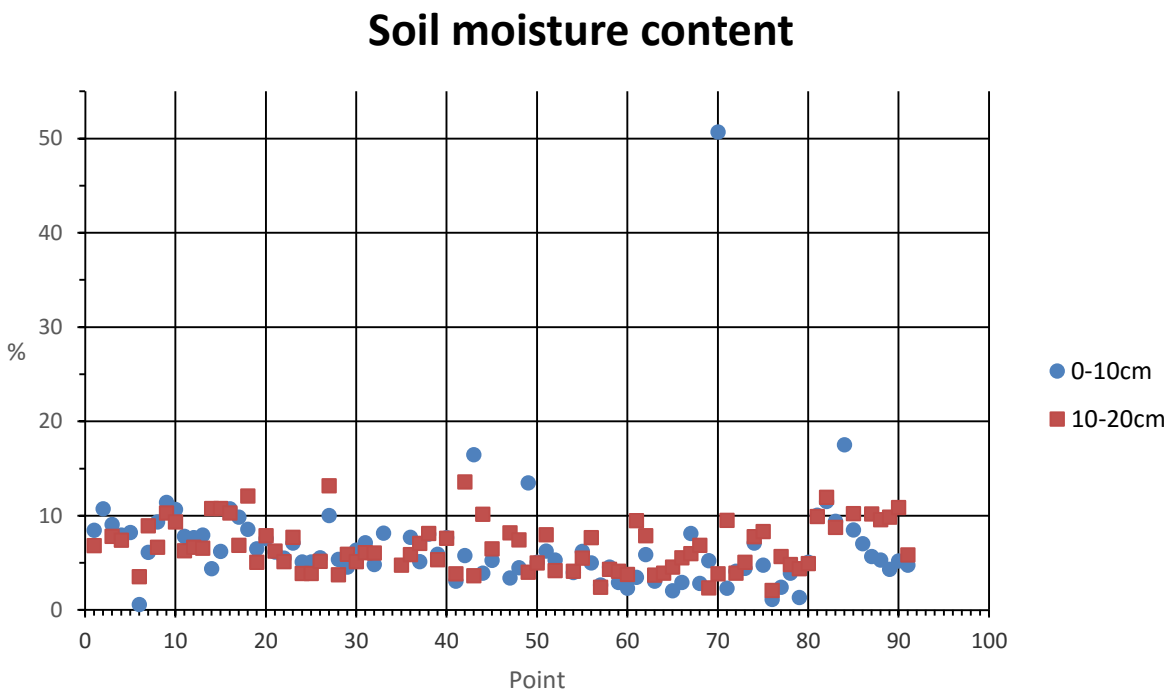

Figure 23: Soil moisture content at 0-10cm and 10-20cm depth

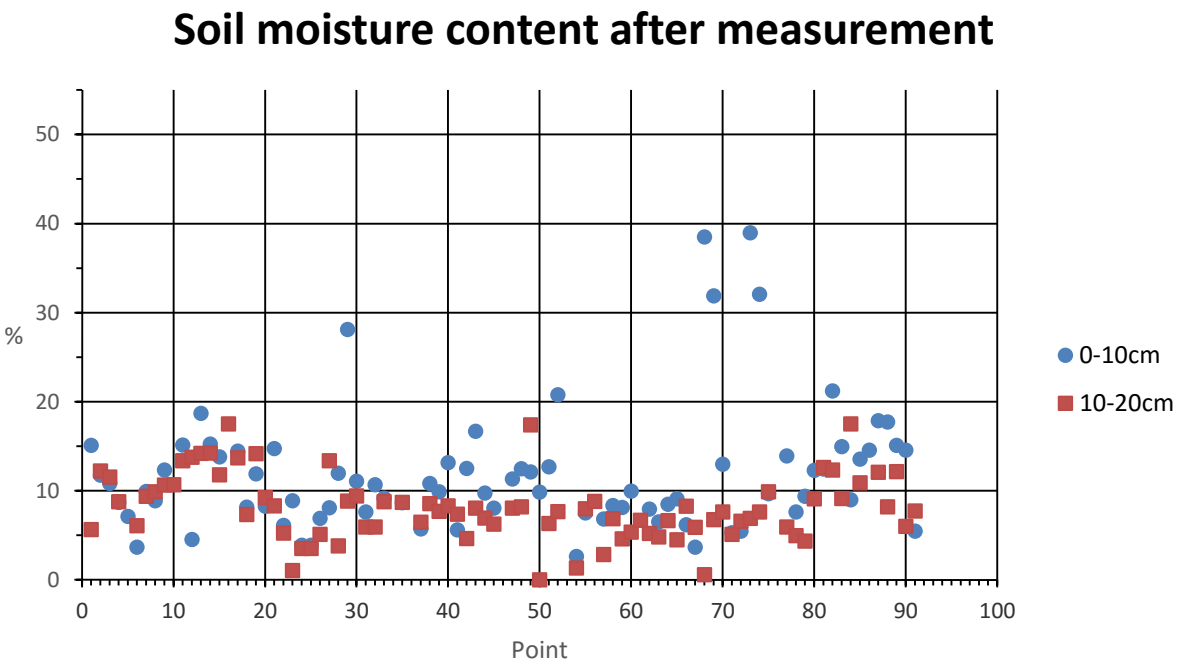

Figure 24: Soil moisture content after measurement at 0-10cm and 10-20cm depth

Descriptive statistics

The mean and standard deviation are shown in table 5.

Table 5: mean values and standard deviations of the soil moisture content

Type and depth	Mean value (%)	Standard deviation (%)
0-10cm	6.55	6.34
10-20cm	6.47	2.49
0-10cm, after measurement	12.45	7.69
10-20cm, after measurement	7.73	3.50

Probability distributions

To ensure that the results were legitimate, they were processed using Matlab to standard probability distribution plots. Because all the data seemed to fit a logarithmic normal distribution, only one example is presented here: soil moisture content at 0-10cm. For more plots see appendix

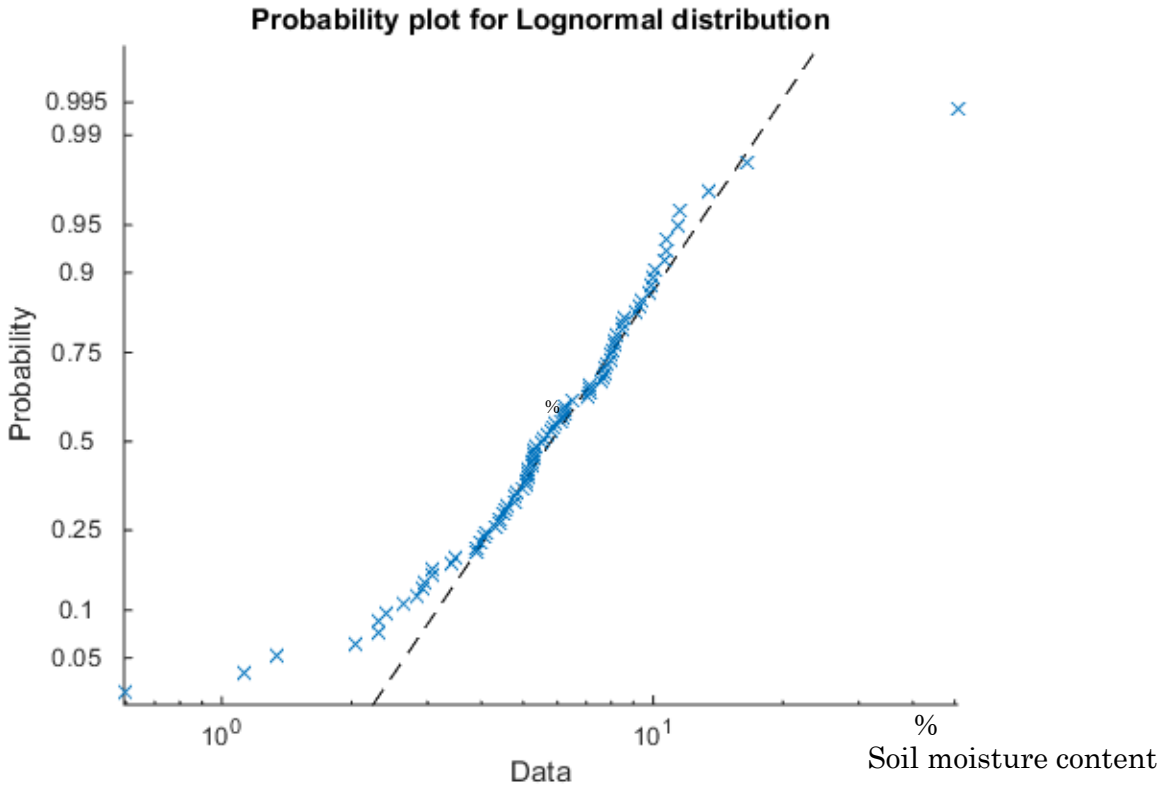

Figure 25: Probability distribution plot for logarithmic normal distribution, for soil moisture content at 0-10cm

Interpolations

The interpolation indicates the spatial variation of the infiltration results. In an effort to simplify comparisons, the color scheme have to a large extent been adjusted to show identical values across the diagrams.

Comparison between different interpolation results

Figure 26 shows the interpolation results for soil moisture content depth 10-20cm. Some of the corners using the spline method are clearly higher and lower than the experiment results. Adding extra virtual points does not solve the problem completely. The kriging interpolation does not show the same tendencies. Similar results can be seen for the other measurements of soil moisture content, see appendix.

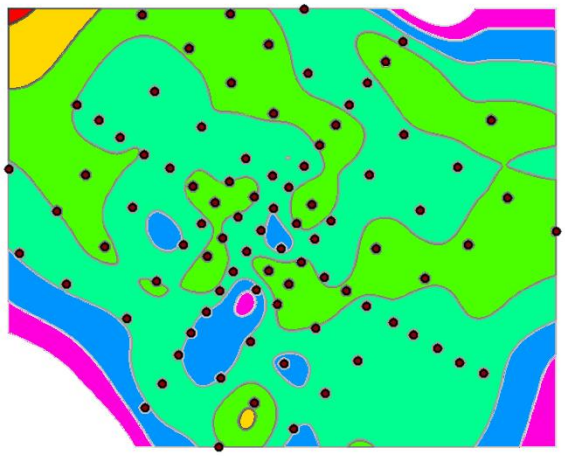

Soil moisture content at 10-20cm using spline

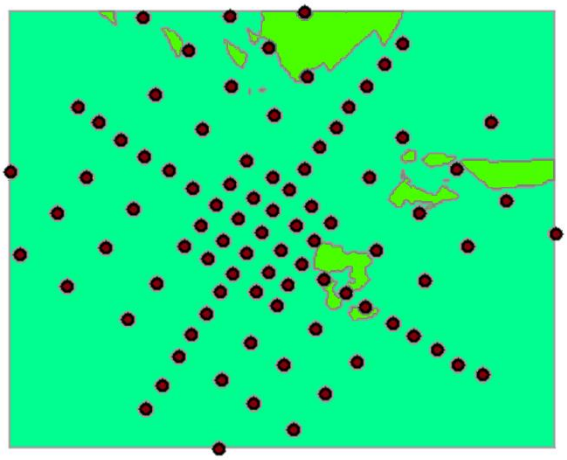

Soil moisture content at 10-20cm using kriging

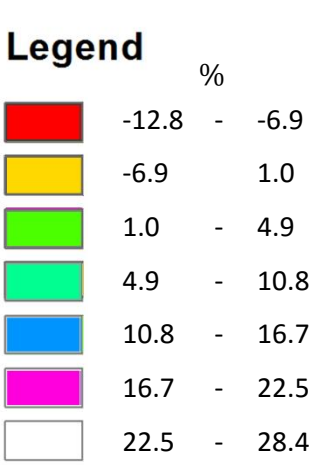

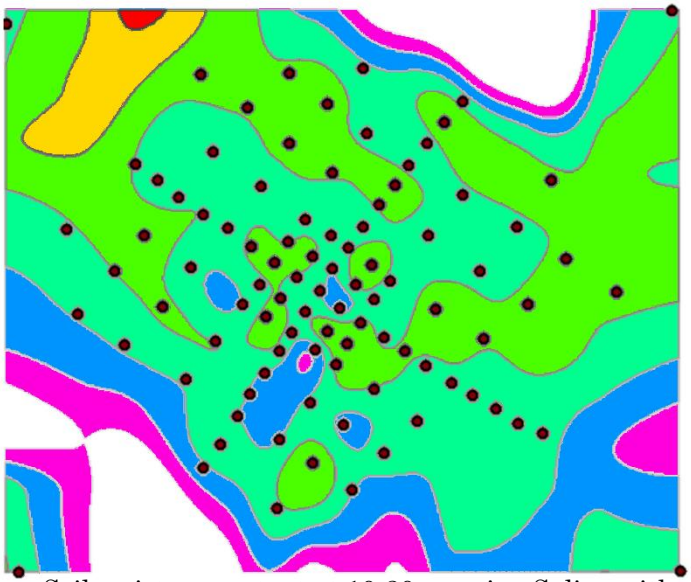

Soil moisture content at 10-20cm using Spline with virtual points

Figure 26: Soil moisture content at 10-20cm with different interpolation methods. Shown are the problems with using the spline interpolation method; with very high or low values near the borders of the area. The problem is not fully re-solved using virtual points outside the area. Kriging does not show these tendencies.

Interpolation results Kriging

Figure 27 shows the spatial variation for the soil moisture content. The soil moisture content at 0-10cm depth was below 15% except for one small area in the north with up to 35%. At 10-20cm depth the values were low with most of the results being 5-10%. After the measurements, at 0-10cm, most of the measurements had a soil moisture content of 5-15%. However there were two distinct spots with higher values in the central north part and central south part. After the measurements, at 10-20cm, most of the points had a soil moisture content of 5-10%, with a slightly larger southwest part.

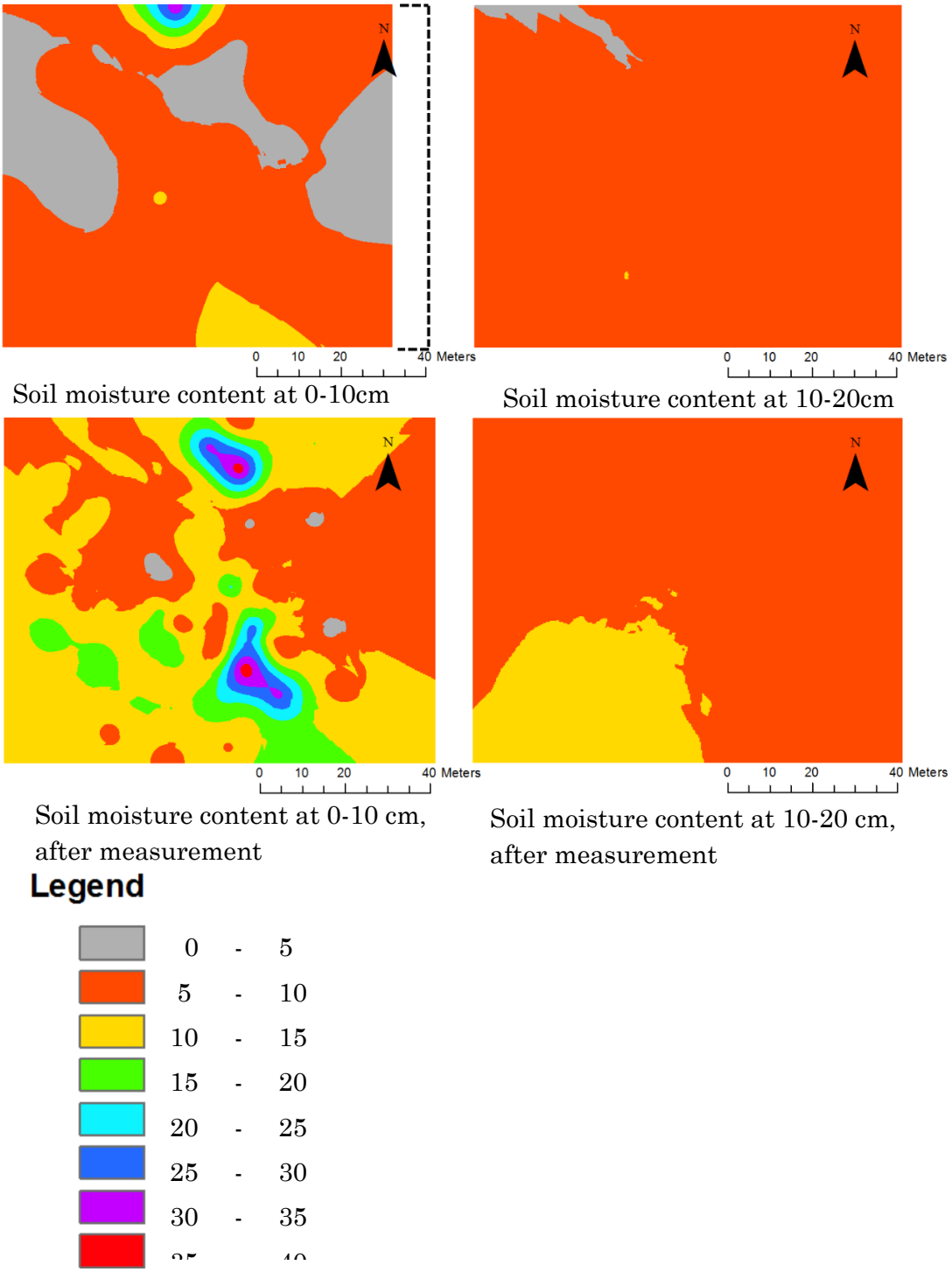

Figure 27: Soil moisture content before and after infiltration measurement.

Comparison

To confirm the results from the interpolation, a selection of the results was plotted against each other. The figures do not show any correlation between the soil moisture content and hydraulic conductivities. Figure 28 shows moisture content at 0-10cm depth versus K1I and K2I. The other comparisons show similar pattern, see appendix.

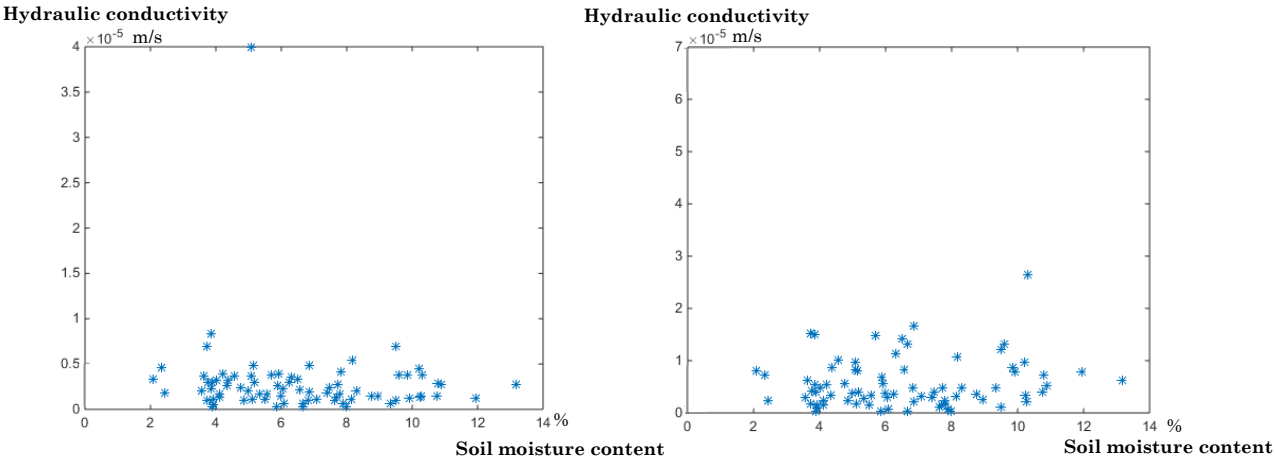

Figure 28: Soil moisture content at 0-10cm depth vs: left a t K1I, right at K2I.

Discussion

Results discussion

Comparing Method I, Method II and Method III

All methods resulted in the need to discard many of the measurements due to negative values. For Method I these values accounted for 23 out of 105 (22%), and for Method II and Method III, 38 out of 105 (36%) and 40 of 105 (38%), respectively. One outlier (point 42) was encountered and discarded.

Even though almost twice the number of values was discarded from Method II and Method III as compared to Method I, all results were in the same range of 10^{-7}-10^{-5} m/s. The mean and standard deviation were also similar, especially for tension h=100 mm. These similarities make it difficult to discern which method that was the most accurate. However while 22% of the results were discarded for Method I this is still the lowest in terms of discarded values. Thus, Method I was deemed as the most the most appropriate. Even so, the large number of discarded measurements does question the usability of the tension infiltrometer altogether as a mean to investigate hydraulic conductivity at different tensions.

Interpolation

The study demonstrated the importance of selecting an appropriate interpolation method. The evaluation was made by comparing the different maps of interpolation. As seen from Figure 18 and 26, the spline interpolation can create erroneous values near the map border. This can be improved by adding virtual points but the spline polynomial still give high error levels where data are scarce. The kriging interpolation did not show the same errors.

Hydraulic conductivity

As mentioned, the hydraulic conductivities were in the range of 10^{-7}-10^{-5} m/s. If compared to the reference values presented in Table 1 it is seen that they correspond to typical values for many soils, in particular silty and sandy soil. However, it is difficult to make a clear comparison because the measurements were performed under tension while the reference values are given without tension. A perhaps better comparison can be made with the saturated hydraulic conductivity which is the hydraulic conductivity for tension h=0, obtained with Method I (see Table 3 and Figure 20). The values of the saturated hydraulic conductivity were about 10 times higher than for the conductivities under tension, but they do still correspond to the same soil types as in Table 1.

Except for the negative values, only one outlier was encountered. In the future, a further comparison can be made using data from similar experiments in the area.

The results did not show any clear connection between the hydraulic conductivity and the soil moisture content or the distance to the river. Instead, the variability of the hydraulic conductivity appears to be a random spatial process.

Soil moisture content

Because the soil moisture content depends on many factors it is no surprise to find a great spatial variation. Selim et al. (2011) came to similar conclusions. Consequently, studies that investigate spatial variation need to choose experimental areas with great care. Also, the time consuming process of investigating infiltration remains and therefore other parameters that can be related to infiltration need to be studied.

Method discussion

Field related considerations

Insufficient hydraulic connection between the infiltrometer and the soil might have affected the measurements. This would cause varying infiltration rate over time that does not reach a constant rate. This was especially clear with Method III. The insufficient hydraulic connection may have been the reason why so many values turned out negative. One reason for this may have been effects of the strong wind during observations.

Another reason why many measurements had to be discarded could be the contact sand with too low hydraulic conductivity. The sand was taken directly from the river bank which may not have been suitable. This is supported by Method III where only 44 of total 105 measurements show effect of the contact sand.

The main disadvantage of the study site was that it was frequently used by people as a recreation site. Trampling may have caused disturbance of the soil, affecting the infiltration and thus the hydraulic conductivity.

The time between the sampling and the analysis of the soil samples might also have been too long.

The application of cumulative infiltration equation

The use of the cumulative infiltration equation, presented here as EQ10, is problematic. On one hand it is intuitive and probably describes the infiltration process very well for natural conditions, e.g., when the rain infiltrates. On the other hand, the measurements using the tension infiltrometer do not reflect natural conditions. Using the contact sand means that a soil with unknown property was used for the early stage infiltration.

Some studies have pointed out that the method of using the cumulative infiltration equation, EQ10, might be more accurate. But it creates more work and many negative results. However, the values found by the constant infiltration rate method were in the same range as the methods using EQ10.

Conclusions

The following general conclusions from the study can be drawn:

- No clear relationships between hydraulic conductivity and soil moisture content were found.
- The simplest and most reliable method of using the tension disc infiltrometer seems to be the Method I.
- The hydraulic conductivities at different tensions spanned a range of 10^{-7}-$10^{-5}\mathrm{m}/s$.

Suggestions for further studies

Because that the two parameter equation gave inconclusive results, more investigation on the physical processes on infiltration should be done to improve instruments and methods.

Even though this study showed similar results as other studies, the main problems with determining infiltration rates remain. Therefore, studies that investigate substitutes for infiltration, or to develop faster and more reliable methods are still very important and research on the subject should continue.

The Bolivian highland, the Altiplano, is an un-researched area thus studies should continue. The studies should be made available through publishing so that future and current investigations can use these.

References

Angulo-Jaramillo, R., Vandervaere, J.P., Roulier, S., Thony, J.L., Gaudet, J.P., Vauclin, M., 2000. Field measurement of soil surface hydraulic properties by disc and ring infiltrometers: A review and recent developments. *Soil & Tillage Research,* Volume 55, pp. 1-29.

Ankeny, M., Ahmed, M., Kaspar, T. & Horton, R., 1991. Simple field method for determining unsaturated hydraulic conductivity. *Soil Sci. Soc. Am. J.,* Issue 55, p. 467470.

ArcGIS, 2014. *ArcGIS.* [Online]
Available at:
https://www.arcgis.com/home/webmap/viewer.html?layers=45b49382f21c481c972649d1137a2d7c
[Accessed 15 10 2014].

BBC, 2015. *Mundo.* [Online]
Available at:
http://www.bbc.com/mundo/ultimas_noticias/2015/02/150227_ultnot_uruguay_bolivia_acuerdo_puerto_egn
[Accessed 07 07 2015].

Benchwick, G. & Smith, P., 2013. *Lonely planet Bolivia.* 8 ed. China: Lonely planet publications Pty Lth.

Brutsaert, W., 2005. *Hydrology, an introduction.* [Online]
Available at:
http://ebooks.cambridge.org.ludwig.lub.lu.se/ebook.jsf?bid=CBO9780511808470
[Accessed 30 01 2015].

Calizaya Terceros, A., 2009. *Water resources management efforts for best water allocation in the lake Poopo basin, Bolivia,* Lund: Lund University.

Canaviri Blanco, B. L., 2011. *Tesis de grado, Estimación de la vulnerabilidad intrínseca a la contaminación del acuífero libre en el sistema acuífero de la Challapampa, Oruro mediante análisis comparativo entre los métodos DRASTIC y GOD (S),* Oruro: Universidad Técnica de Oruro, Facultad Nacional de Ingeniería, Sergeotecmin.

Canedo, C., 2014. [Interview] (09 2014).

Canedo, C. & Gomez, E., 2014. *Raindata Oruro 1943-2013.* Oruro: s.n.

CIA, 2015. *CIA world factbook.* [Online]
Available at: https://www.cia.gov/library/publications/the-world-factbook/fields/2147.html
[Accessed 07 07 2015].

Clothier, B., 2004. Soil pores. In: *The Encyclopedia of Soil Science.* The Netherlands: Chestworth, W., Ed..

Dames & Moore Norge, Comibol, 2000. *PMAIM-Subproyecto No. 7. Estudio Hidrogeológico de la Mina San José y los acuíferos que suministran agua a la ciudad de Oruro.,* Oruro: s.n.

Escuela runawasi, language and culture school, 2015. s.l.:s.n.

ESRI, 2012. *Arcgis help 10.1.* [Online]
Available at:
http://resources.arcgis.com/en/help/main/10.1/index.html#//009z00000078000000
[Accessed 10 08 2015].

Esri, 2014. *ArcGIS help 10.2.* [Online]
Available at:
http://resources.arcgis.com/en/help/main/10.2/index.html#//009z00000076000000
[Accessed 21 01 2015].

Fetter, C., 2001. *Applied hydrogeology.* 4:th ed. New Jersey: Prentice-Hall inc.

Gardner, W., 1958. Some steady state solutions of unsaturated moisture flow equations with application to evaporation from a water table. *Soil Science,* Volume 85, p. 228232.

Geobol & Swedish Geological AB, 1992. *Carta geológica de Bolivia - hoja Oruro,* s.l.: Publicación SGB Serie I-CGB-11.

Goix, S., Point, D., Priscia, O., Polve, P., Duprey, J.L., Mazurek, H., 2011. Influence of source distribution and geochemical composition of aerosols on children exposure in the large polymetallic mining region of the Bolivian Altiplano. *Science of the Total Environment,* pp. 170-184.

Gomez, E., 2014. *Manuscript for PhD course: overview of existing data and previous investigations.* s.l.:s.n.

Google Inc, 2015. *Google Earth,* Paria: Google Inc.

Google, 2015. *Google maps.* [Online]
Available at: https://www.google.se/maps/place/Mina+San+Jos%C3%A9/@-17.9564161,-67.0943647,12z/data=!4m2!3m1!1s0x93e2b09ea647b83b:0x4f1fb90feebb4125
[Accessed 2 april 2015].

Haverkamp, R., Ross, P. & Smettem, K. R. J., 1994. Three-dimenisional analysis of infiltration from the disc infiltrometer. *Water resources research,* 30(11), pp. 2931-2935.

IPCC, 2014. *Climate change 2014: Synthesis report,* s.l.: s.n.

Ivarsson, C. & Lindström, J., 2015. *Hydrological properties of the Azanaque river basin in view of flooding problems,* Lund: Lund University.

Johnson, A., 1963. *A field method for measurement of infiltration, Geological survey water-supply paper 1544-F,* Washington: United States government printing office.

Kirkham, M., 2005. Infiltration. In: *Principles of soil and plant water relations.* s.l.:Elsevier Inc, pp. 145-172.

Mehta, L., Allouche, J., Nicol, A. & Walnycki, A., 2014. Global environmental justice and the right to water: The case of peri-urban Cochabamba and Delhi. *Geoforum,* Volume 54, pp. 158-166.

Mesa Gisbert, C., de Mesa, J. & Gisbert, T., 2012. *Historia de Bolivia.* 8 ed. La Paz: Papeleria y Editorial Gisbert y Cia. S.A..

Nationalencyklopedin, 2015. *Bolivia.* [Online]
Available at: http://www.ne.se/uppslagsverk/encyklopedi/lång/bolivia
[Accessed 29 01 2015].

Oxfam International, 2009. *Bolivia climate change, poverty and adaptation Executive summary,* s.l.: Oxfam International.

Ramos, O. Rötting, T.S., French, M., Sracek, O., Bundschuh, J., Quintanilla, J., Bhattacharya, P., 2014. Geochemical processes controlling mobilization of arsenic and trace elements in shallow aquifers and surface aters in the Antequera and Poopò mining regions, Bolivian Altiplano. *Journal of Hydrology,* Volume 518, pp. 421-433.

Schosinsky, G. & Losilla, M., 2000. Modelo analítico para determinar la infiltración. *Revista Geológica de América Central,* Volume 23, pp. 43-55.

Selim, T., Berndtsson, R., Persson, M., Bouksila, F., Aljaradin, M., 2011. Spatial analysis of infiltration experiment. *Australian Journal of Basic and Applied Sciences,* pp. 729-742.

Servicio Nacional de Meterología e Hidrología, Bolivia, 2015. *SISMET.* [Online]
Available at: http://www.senamhi.gob.bo/sismet/index.php
[Accessed 27 08 2015].

SIDA, 2014. *Vårt arbete i Bolivia.* [Online]
Available at: http://www.sida.se/Svenska/Har-arbetar-vi/Latinamerika/Bolivia/Vart-arbete-i-Bolivia/

SMHI, 2015. *Klimatindikator - nederbörd.* [Online]
Available at: http://www.smhi.se/klimatdata/meteorologi/nederbord/klimatindikator-nederbord-1.2887
[Accessed 14 08 2015].

Soil Measurement Systems, 2015. *Mail conversation.* s.l.:s.n.

Soilmoisture equipment corp., 2008. *2826D20 Operating instructions.* Santa Barbara: Soilmoisture Equipment Corp.

Svenska Dagbladet, 2009. *Svenska Dagbladet.* [Online]
Available at: http://www.svd.se/litium-ar-bolivias-vita-guld
[Accessed 22 10 2015].

US department of state, 2014. *US department of state.* [Online]
Available at: http://www.state.gov/r/pa/ei/bgn/35751.htm
[Accessed 07 07 2015].

US Geological Survey, 2015. *the Water cycle - USGS Water science school.* [Online]
Available at: http://water.usgs.gov/edu/watercycleinfiltration.html
[Accessed 14 08 2015].

Vandervaere, J., Vauclin, M. & Elrick, D., 2000. Transient flow from tension infiltrometers: i. the Two-parameter equation. *Soil Sci. Soc. Am. J.,* Volume 64, p. 1263–1272.

Warrick, A., 1992. Models for disc infiltrometers.. *Water resour. Res.,* Volume 28, pp. 1319-1327.

Wikipedia, 2014. *Wikipedia.* [Online]
Available at: http://en.wikipedia.org/wiki/Oruro,_Bolivia

Wooding, R., 1968. Steady infiltration from a shallow circular pond. *Water Resoure Res,* Volume 4, pp. 1259-1273.

Zhang, R., 1997b. Infiltration models for the disc infiltrometer. *Soil Sci. Soc. Am. J.,* Volume 61, pp. 1597-1603.

Zhang, R., 1998. Estimating hydraulic conductivity and macroscopic capillary length from the disc infiltrometer. *Soil Sci. Soc. Am. J.,* Volume 62, pp. 1513-1521.

Appendix

Statistical data

Hydraulic conductivity

Method I

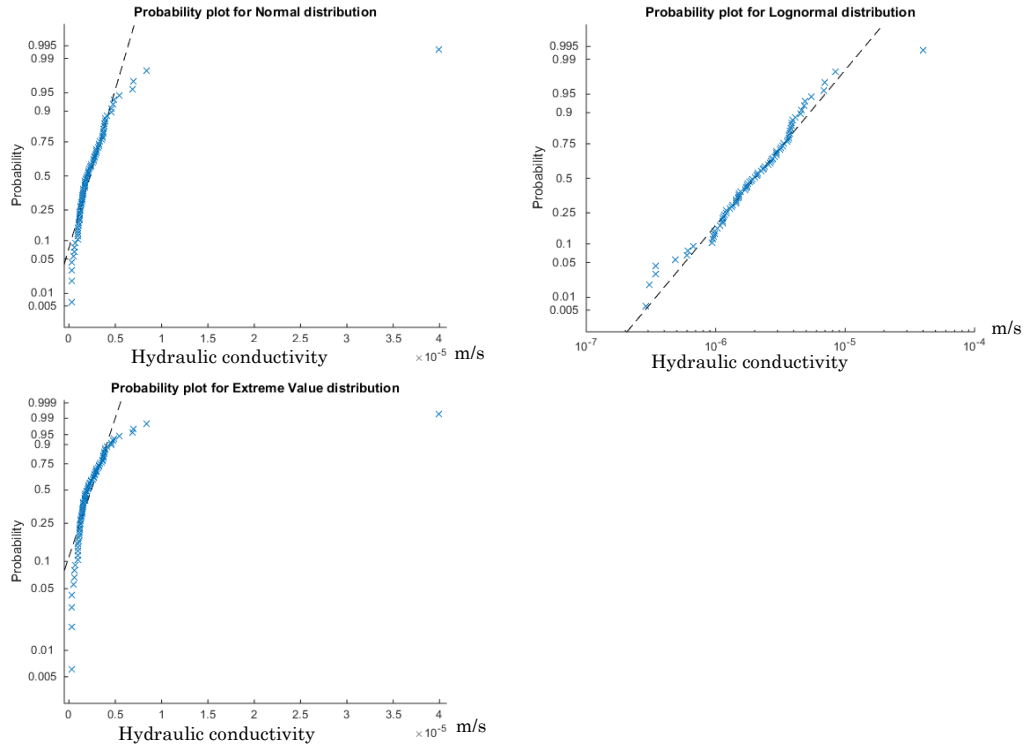

Figure 29: Probability distribution plots for K1I.

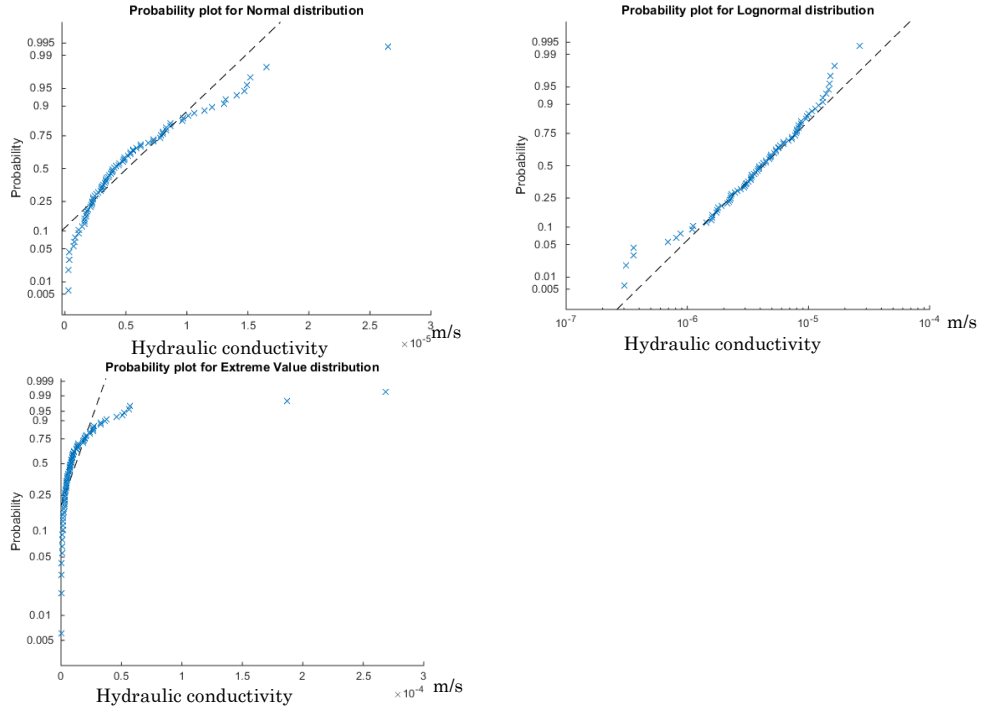

Figure 30: Probability distribution plots for K2I

Method II

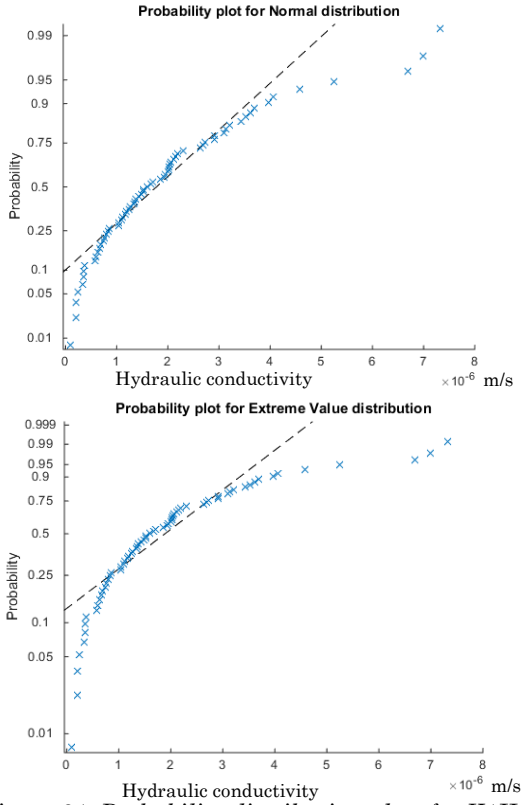

Figure 31: Probability distribution plots for K1II

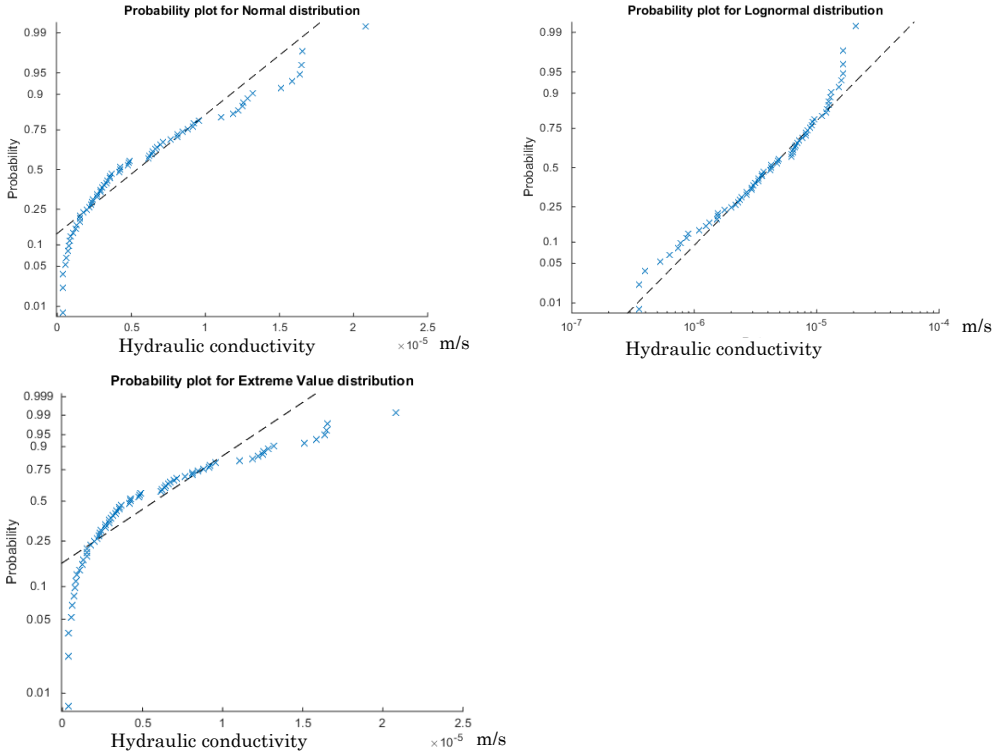

Figure 32: Probability distribution plots for K2II

Method III

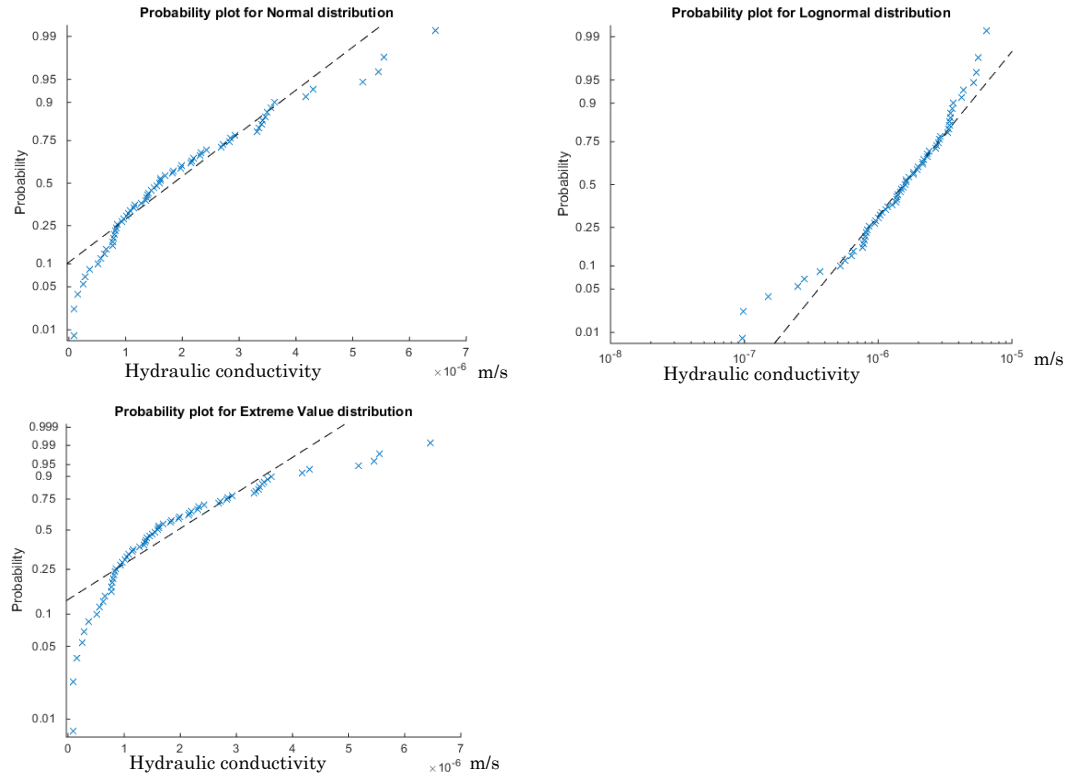

Figure 33: Probability distributions plots for K1III

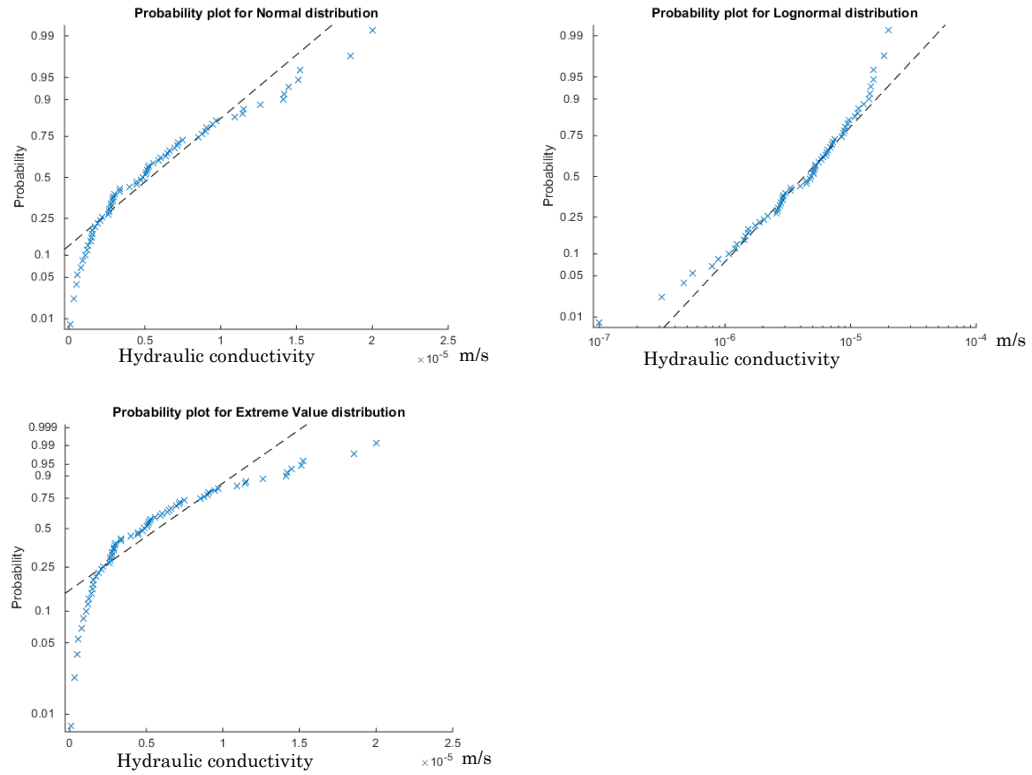

Figure 34: Probability distributions plots for K1III

Soil moisture content at 0-10cm

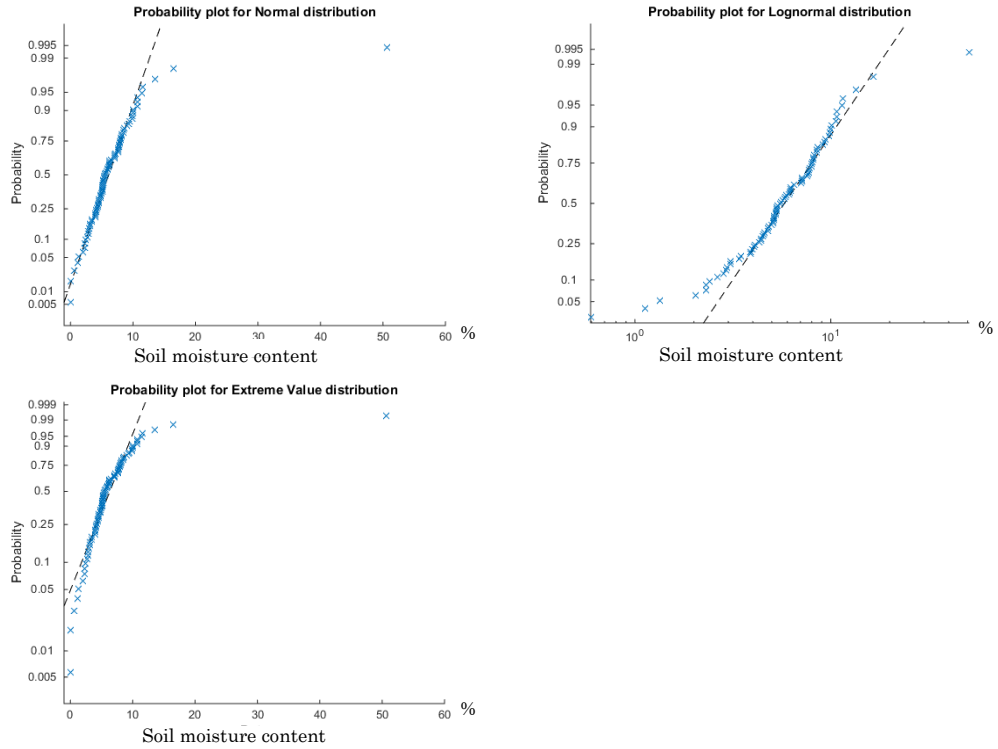

Figure 35: Probability distribution plots for soil moisture content at 0-10cm depth, in percentage water of weight.

Soil moisture content at 10-20cm depth

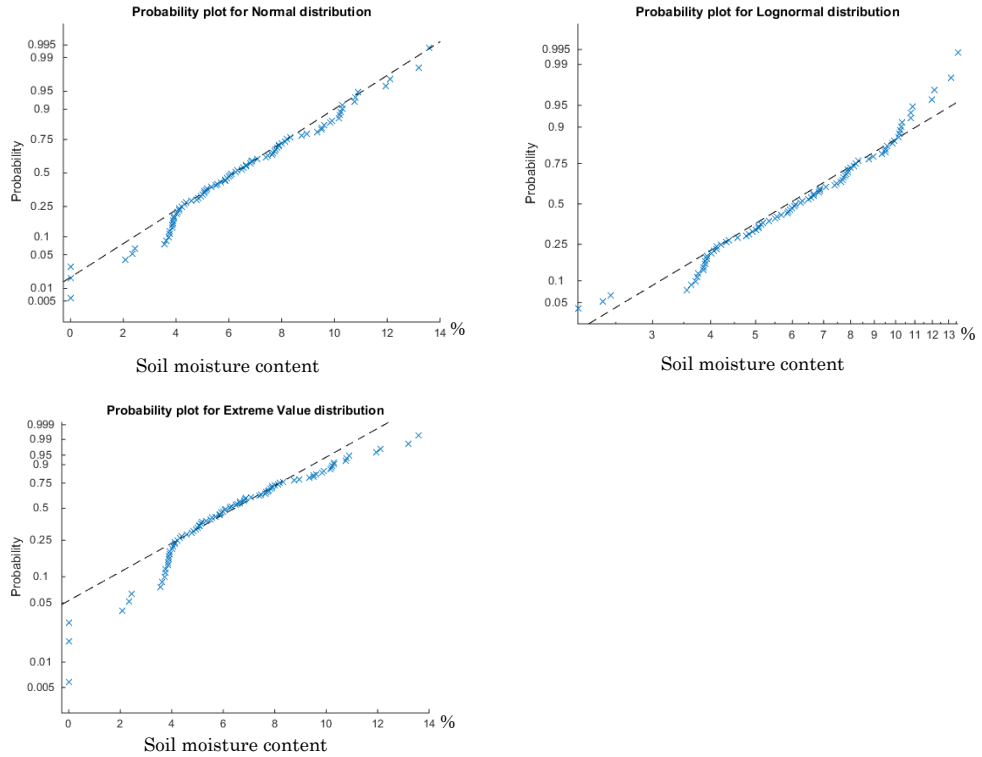

Figure 36: Probability distribution plots for soil moisture content at 10-20cm depth, in percentage water of weight

Soil moisture content at 0-10cm after measurement

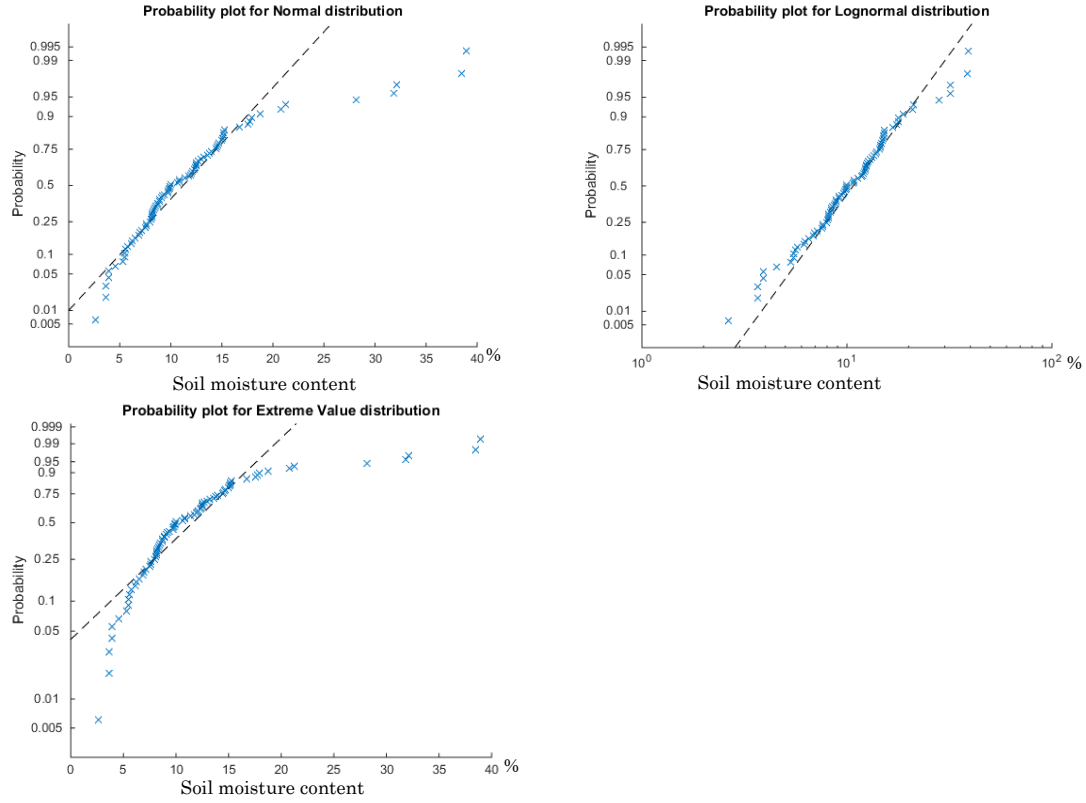

Figure 37: Probability distribution plots for soil moisture content after measurement, at 0-10cm depth, in percentage water of weight.

Soil moisture content 10-20cm after measurement

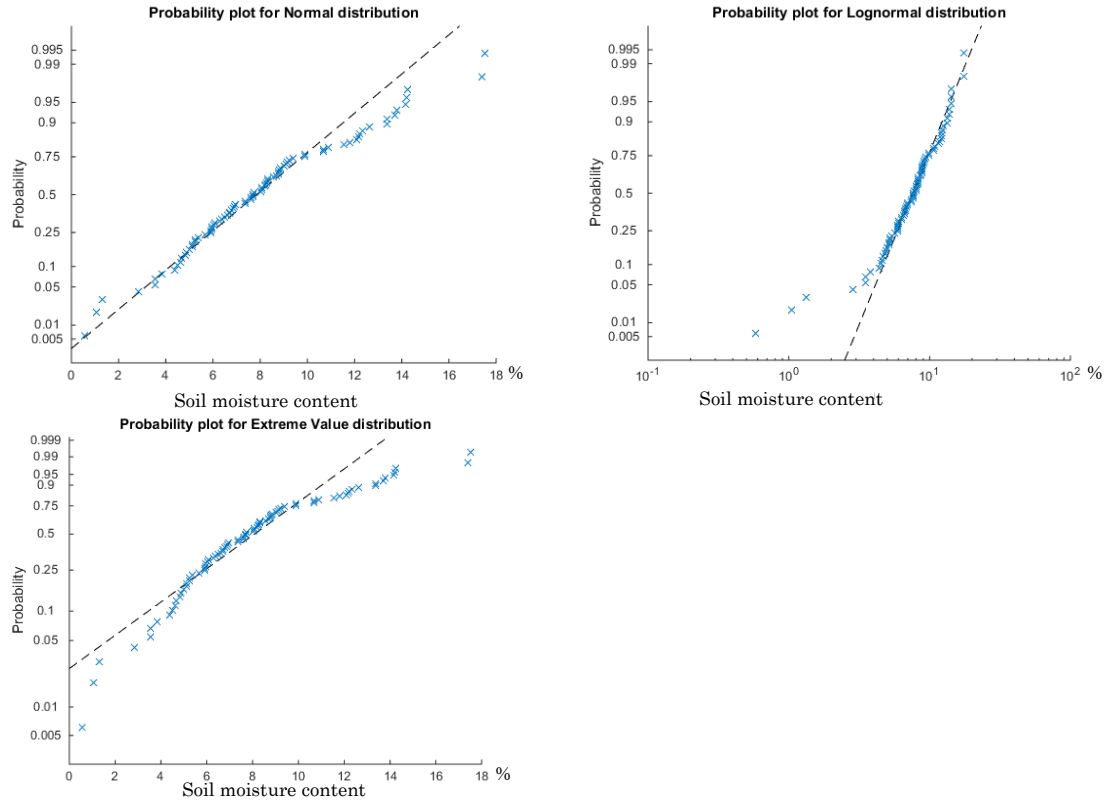

Figure 38: Probability distribution plots for soil moisture content after measurement, at 10-20cm depth, in percentage water of weight.

Comparison

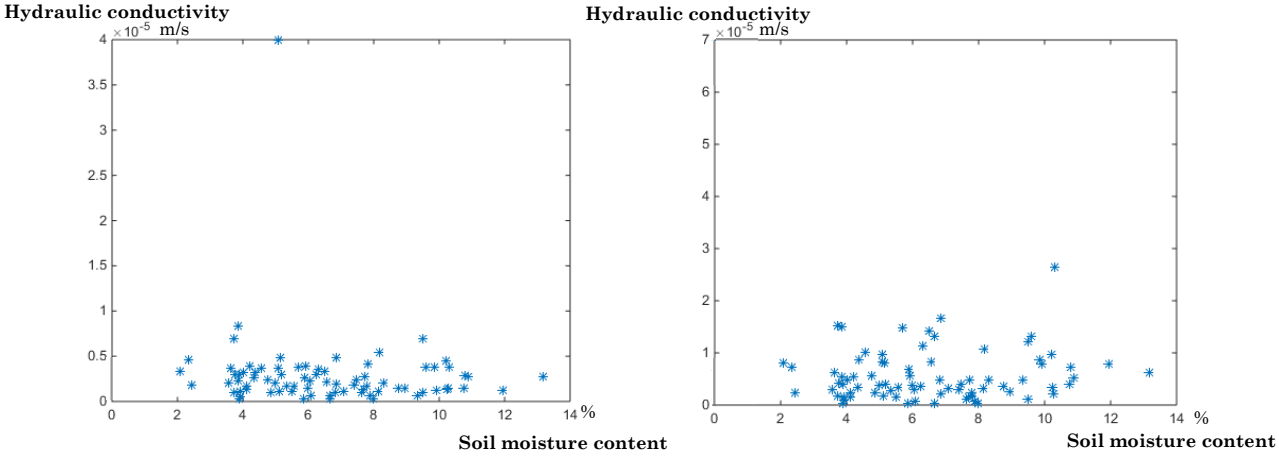

Figure 39: moisture content at 0-10cm depth vs hydraulic conductivity: left at K1I, right at K2I

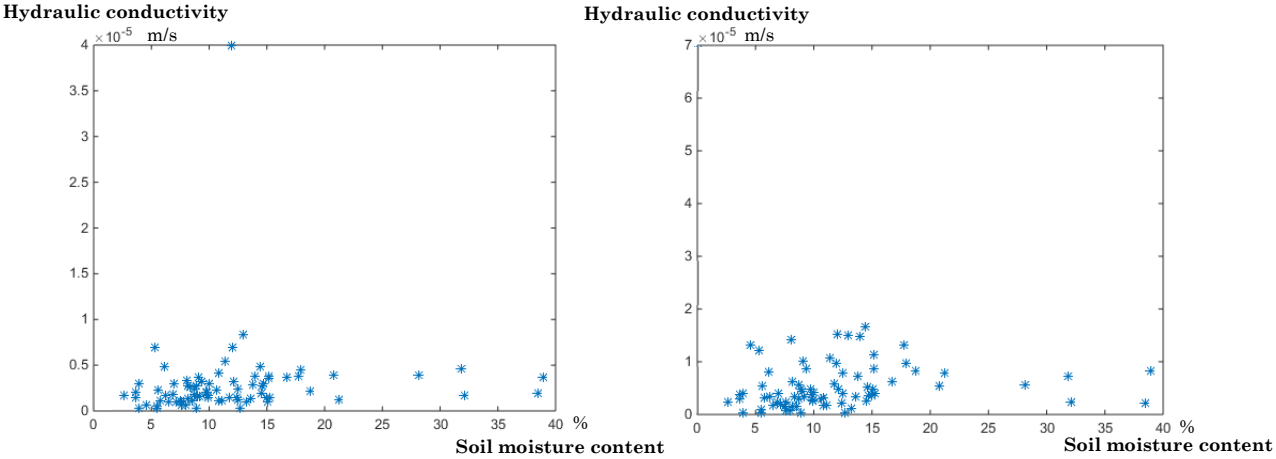

Figure 40: moisture content at 10-20cm depth vs: left at K1I, right at K2I

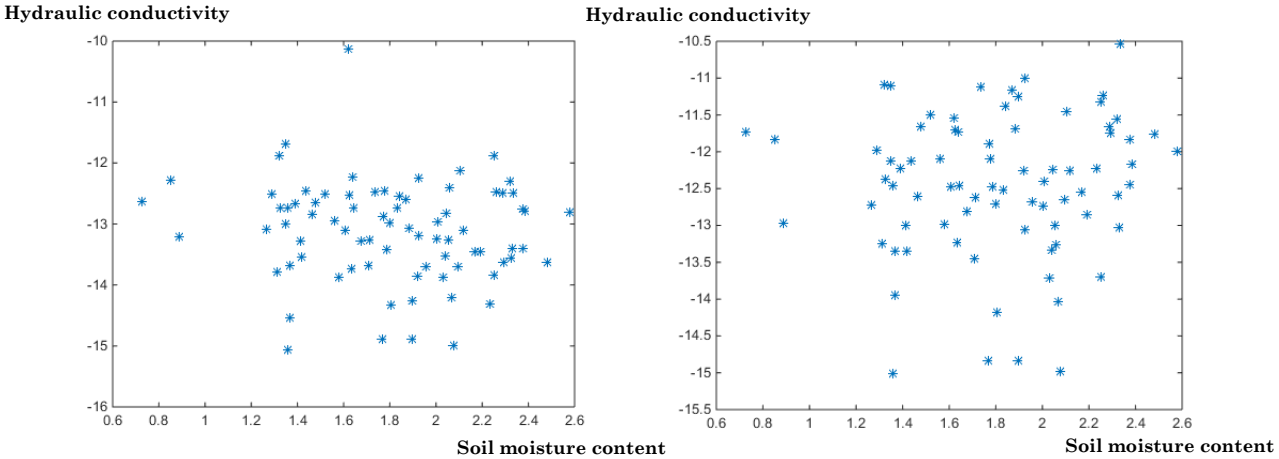

Figure 41: natural logarithm of moisture content at 0-10cm depth vs, natural logarithm of hydraulic conductivity: left at K1I, right at K2I

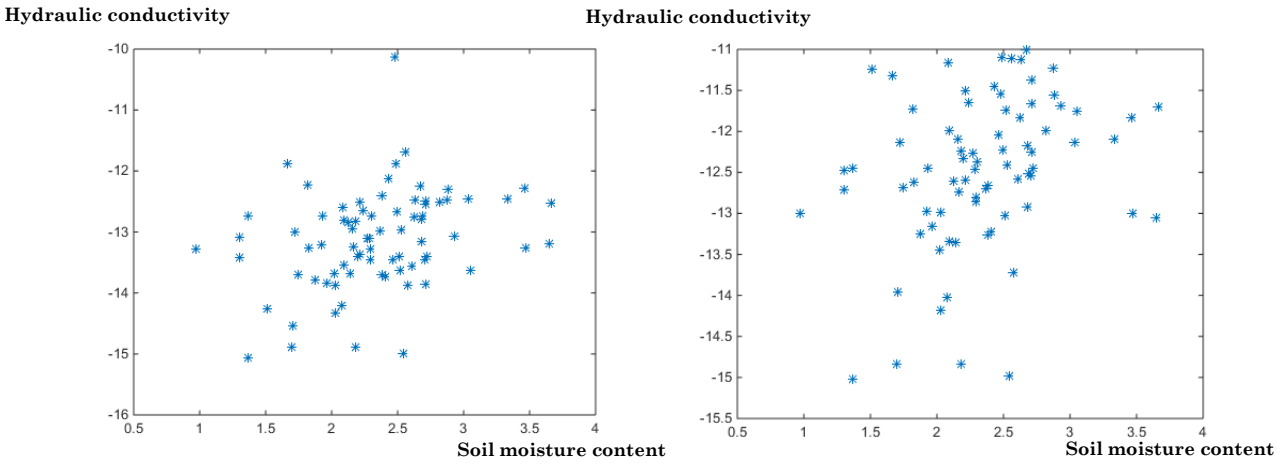

Figure 42: Natural Logarithm of moisture content at 10-20cm depth vs, natural logarithm of hydraulic conductivity: left at K1I, right at K2I

Hydraulic conductivity data in m/s

Point	K1I	K2I	K0I	K1II	K2II	K1III	K2III
Point1	9.59E-07	4.78E-06	3.87E-06	Hydraulic conductivities for Point1, Point2 and Point 12 were measured at different tensions and then recalculated with EQ4 for tensions h=-100 and h=-50			
Point2	1.43E-06	5.87E-06	4.87E-06				
Point3	4.09E-06	1.74E-06	1.94E-06	3.10E-06	1.54E-06	0.0744	2.72E-06
Point4	1.76E-06	2.95E-06	2.76E-06	2.92E-05	1.42E-05	-0.0723	3.69E-07
Point5	9.78E-07	1.92E-06	1.76E-06	1.03E-06	2.17E-06	0.0706	1.04E-06
Point6	2.07E-06	3.00E-06	2.86E-06	1.37E-06	3.14E-06	0.064	4.07E-05
Point7	1.44E-06	2.60E-06	2.40E-06	7.94E-07	2.29E-06	0.0597	6.33E-07
Point8	3.41E-07	3.59E-07	3.57E-07	2.49E-07	2.69E-06	0.0295	-8.45E-07
Point9	1.51E-06	2.20E-06	2.09E-06	7.40E-07	8.59E-07	2.20E-06	1.08E-06
Point10	6.12E-07	4.89E-06	3.72E-06	8.45E-07	4.23E-06	0.0188	5.19E-07
Point11	3.55E-06	1.14E-05	9.80E-06	3.21E-06	1.29E-05	0.0237	3.46E-06
Point12	6.40E-07	1.31E-05	8.80E-06	-	-	-	-
Point13	2.11E-06	8.34E-06	6.96E-06	2.03E-06	8.10E-06	0.0185	1.84E-06
Point14	1.51E-06	3.90E-06	3.45E-06	1.16E-06	4.20E-06	0.0442	-1.09E-06
Point15	2.87E-06	7.26E-06	6.42E-06	2.63E-06	6.44E-06	0.0595	2.20E-06
Point16	3.76E-06	2.65E-05	2.05E-05	1.71E-06	2.08E-05	0.0295	2.33E-06
Point17	4.79E-06	1.65E-05	1.41E-05	4.06E-06	1.58E-05	0.0423	4.17E-06
Point18	-1.70E-06	-1.62E-06	-1.63E-06	1.18E-06	1.24E-06	1.0715	-4.80E-07
Point19	3.99E-05	9.73E-06	1.17E-05	4.04E-05	3.99E-05	-0.0389	4.33E-05
Point20	-7.41E-07	-7.20E-07	-7.23E-07	2.92E-06	9.22E-06	0.0482	4.31E-06
Point21	2.92E-06	3.66E-06	3.56E-06	1.96E-06	9.18E-06	0.0385	3.31E-06
Point22	4.89E-06	8.03E-06	7.52E-06	2.02E-06	1.22E-05	0.0349	3.49E-06
Point23	2.69E-06	4.81E-06	4.46E-06	2.19E-06	3.36E-06	0.1183	8.29E-07
Point24	2.93E-06	3.90E-06	3.75E-06	3.45E-07	3.54E-07	1.9691	2.14E-06
Point25	2.86E-07	3.01E-07	2.99E-07	-2.46E-06	-1.93E-06	-0.207	-3.97E-07
Point26	2.93E-06	3.90E-06	3.75E-06	3.45E-07	3.54E-07	1.9691	2.14E-06
Point27	2.73E-06	6.22E-06	5.58E-06	2.11E-06	3.54E-06	0.0985	2.42E-06
Point28	6.98E-06	1.52E-05	1.37E-05	4.57E-06	1.65E-05	0.0441	5.18E-06
Point29	3.90E-06	5.61E-06	5.35E-06	2.69E-06	3.32E-06	0.2392	3.39E-06
Point30	1.08E-06	1.80E-06	1.68E-06	1.03E-06	1.77E-06	0.0953	8.59E-07
Point31	5.99E-07	6.93E-07	6.80E-07	-9.56E-07	-8.21E-07	-0.3279	9.71E-08
Point32	2.31E-06	3.04E-06	2.93E-06	2.30E-06	4.80E-06	0.0709	2.69E-06
Point33	1.55E-06	3.38E-06	3.05E-06	-2.37E-06	4.44E-06	0.0076	-1.69E-06
Point34	1.44E-04	6.90E-05	7.60E-05	-3.27E-05	-2.16E-05	-0.1227	2.67E-05
Point35	2.38E-06	5.62E-06	5.02E-06	2.02E-06	4.23E-06	0.0708	1.70E-06
Point36	2.57E-06	6.85E-06	6.02E-06	2.00E-06	6.62E-06	0.0466	1.62E-06
Point37	1.12E-06	3.10E-06	2.71E-06	-1.40E-06	4.22E-06	-0.0129	-3.28E-06
Point38	1.12E-06	3.19E-06	2.78E-06	1.11E-06	2.66E-06	0.0605	9.62E-07
Point39	1.71E-06	2.74E-06	2.58E-06	1.66E-06	2.94E-06	0.09	1.50E-06
Point40	9.44E-07	1.10E-06	1.08E-06	1.09E-06	1.33E-06	0.2586	1.35E-06
Point41	2.25E-06	5.38E-06	4.80E-06	2.05E-06	4.89E-06	0.0173	1.82E-06

Point42	2.72E-01	1.83E-05	6.47E-05	3.49E-01	2.61E-05	-0.025	3.01E-01
Point43	3.67E-06	6.23E-06	5.81E-06	3.43E-06	6.17E-06	0.0877	3.35E-06
Point44	-5.91E-21	-5.91E-21	-5.91E-21	5.78E-07	6.29E-07	0.5895	7.65E-07
Point45	3.35E-06	1.41E-05	1.17E-05	2.91E-06	1.64E-05	0.0358	2.31E-06
Point46	-1.83E-05	-1.19E-05	-1.26E-05	-3.04E-06	5.17E-06	0.0065	-1.37E-05
Point47	5.43E-06	1.06E-05	9.73E-06	3.70E-06	1.32E-05	0.0444	3.62E-06
Point48	2.35E-06	4.08E-06	3.79E-06	1.93E-06	3.66E-06	0.0809	1.60E-06
Point49	3.15E-06	4.87E-06	4.60E-06	1.86E-06	2.36E-06	0.2095	1.98E-06
Point50	2.02E-06	3.85E-06	3.54E-06	6.90E-07	7.43E-07	0.6807	1.61E-06
Point51	3.08E-07	3.12E-07	3.12E-07	6.69E-06	1.19E-05	0.0361	5.45E-06
Point52	3.87E-06	5.38E-06	5.16E-06	3.52E-06	8.79E-06	0.0584	3.41E-06
Point53	-6.06E-06	-4.60E-06	-4.77E-06	-1.52E-05	-9.98E-06	-0.1214	-7.03E-06
Point54	1.69E-06	2.26E-06	2.18E-06	1.26E-06	1.56E-06	0.0162	1.40E-06
Point55	1.15E-06	1.44E-06	1.40E-06	6.23E-07	7.72E-07	0.2342	7.71E-07
Point56	1.35E-06	1.62E-06	1.58E-06	1.60E-06	2.43E-06	0.1224	1.38E-06
Point57	1.83E-06	2.33E-06	2.25E-06	3.79E-07	3.95E-07	1.2286	1.17E-06
Point58	2.65E-06	3.36E-06	3.26E-06	1.52E-06	7.13E-06	0.0083	1.55E-06
Point59	1.32E-06	1.60E-06	1.56E-06	-1.27E-06	3.95E-06	0.0129	-1.31E-06
Point60	2.96E-06	4.23E-06	4.03E-06	1.34E-06	6.74E-06	0.0374	1.97E-06
Point61	9.79E-07	1.12E-06	1.10E-06	1.42E-06	2.94E-06	0.0719	1.27E-06
Point62	6.73E-07	8.08E-07	7.89E-07	8.36E-07	1.10E-06	0.1845	8.02E-07
Point63	1.02E-06	1.77E-06	1.65E-06	6.65E-07	8.98E-07	0.1673	5.66E-07
Point64	1.14E-06	1.59E-06	1.52E-06	1.24E-06	2.00E-06	0.1067	1.01E-06
Point65	3.70E-06	1.01E-05	8.85E-06	1.97E-07	1.11E-05	0.0259	7.87E-07
Point66	1.73E-06	3.32E-06	3.05E-06	-1.50E-06	4.70E-06	0.0129	-6.47E-07
Point67	1.49E-06	3.79E-06	3.35E-06	1.36E-06	3.03E-06	0.0658	1.14E-06
Point68	1.87E-06	2.14E-06	2.10E-06	2.73E-06	6.20E-06	0.0642	2.82E-06
Point69	4.62E-06	7.29E-06	6.87E-06	3.96E-06	9.57E-06	0.0483	3.57E-06
Point70	8.36E-06	1.50E-05	1.39E-05	7.33E-06	1.65E-05	0.065	5.55E-06
Point71	6.90E-06	1.20E-05	1.12E-05	6.98E-06	1.25E-05	0.0878	6.45E-06
Point72	4.84E-07	8.71E-07	8.07E-07	3.33E-07	5.27E-07	0.1108	2.82E-07
Point73	3.64E-06	8.31E-06	7.45E-06	3.61E-06	8.12E-06	0.0649	2.93E-06
Point74	1.75E-06	2.27E-06	2.19E-06	1.48E-06	4.78E-06	0.0473	1.37E-06
Point75	2.02E-06	4.72E-06	4.23E-06	-1.46E-06	6.16E-06	0.0154	-8.78E-07
Point76	3.28E-06	8.01E-06	7.12E-06	1.53E-06	7.66E-06	0.0375	1.46E-06
Point77	3.83E-06	1.47E-05	1.23E-05	2.16E-06	1.51E-05	0.0375	2.16E-06
Point78	9.41E-07	2.29E-06	2.04E-06	7.67E-07	1.55E-06	8.25E-04	6.53E-07
Point79	3.20E-06	8.68E-06	7.61E-06	3.14E-06	8.48E-06	0.0545	2.84E-06
Point80	-5.32E-06	-3.99E-06	-4.14E-06	-2.45E-06	-1.99E-06	-0.2425	-9.02E-07
Point81	1.21E-06	7.91E-06	6.18E-06	2.10E-07	6.97E-06	0.0266	1.51E-07
Point82	1.20E-06	7.82E-06	6.12E-06	5.25E-06	3.54E-06	0.014	-1.80E-06
Point83	1.43E-06	3.57E-06	3.16E-06	-1.51E-06	5.35E-06	0.014	-1.72E-06
Point84	1.52E-06	4.43E-06	3.85E-06	-5.01E-06	6.25E-06	0.0027	-4.65E-06
Point85	1.28E-06	3.42E-06	3.01E-06	-1.83E-06	4.51E-06	0.0106	-1.75E-06

Point86	1.92E-06	2.45E-06	2.38E-06	-4.11E-07	5.97E-06	0.0218	9.36E-07
Point87	4.53E-06	9.61E-06	8.70E-06	5.85E-07	1.25E-05	0.0275	8.13E-07
Point88	3.80E-06	1.32E-05	1.12E-05	-6.86E-07	1.52E-05	0.0228	9.84E-08
Point89	3.76E-06	8.64E-06	7.74E-06	-1.60E-06	1.25E-05	0.0193	-1.10E-06
Point90	2.78E-06	5.19E-06	4.78E-06	9.91E-08	6.39E-06	0.0258	2.50E-07
Point91	3.41E-07	3.61E-07	3.58E-07	-2.63E-06	3.70E-06	0.0042	-7.66E-07

Soil moisture content

Point	0-10cm	10-20cm	0-10cm after measurement	10-20cm after measurement
Point1	8.461643	6.826282	15.09529	5.647158
Point2	10.74827	0	11.78018	12.21879
Point3	9.080865	7.828735	10.84612	11.53486
Point4	7.954601	7.406359	8.727405	8.769892
Point5	8.236429	-	7.122866	-
Point6	0.594034	3.548628	3.682953	6.072319
Point7	6.141744	8.948394	9.93878	9.411599
Point8	9.333403	6.654942	8.878647	9.898755
Point9	11.43446	10.28922	12.35733	10.66915
Point10	10.67756	9.351291	-	10.68596
Point11	7.819871	6.31158	15.13682	13.39246
Point12	7.700319	6.658648	4.539863	13.78209
Point13	7.956964	6.565755	18.72083	14.22436
Point14	4.382275	10.76789	15.25966	14.24278
Point15	6.237646	10.78999	13.81883	11.79917
Point16	10.75278	10.30992	-	17.51679
Point17	9.850981	6.869137	14.46598	13.7196
Point18	8.581919	12.09947	8.159034	7.360686
Point19	6.492894	5.067634	11.91895	14.16771
Point20	7.597004	7.891723	8.276711	9.246224
Point21	6.16908	6.25006	14.7406	8.304981
Point22	5.511897	5.146001	6.139272	5.24519
Point23	7.123219	7.733888	8.880266	1.040895
Point24	5.119137	3.890073	3.911495	3.525694
Point25	5.119137	3.890073	3.911495	3.525694
Point26	5.548397	5.176954	6.9228	5.112916
Point27	10.02572	13.18912	8.117906	13.38591
Point28	5.376043	3.740883	11.99031	3.826093
Point29	4.553102	5.924577	28.11971	8.847947
Point30	6.365897	5.127285	11.06919	9.43507
Point31	7.15117	6.084515	7.627769	5.962003
Point32	4.838699	6.051115	10.69008	5.962631
Point33	8.1787	-	9.180652	8.766676
Point34	-	-	-	-
Point35	-	4.76736	8.67419	8.695031
Point36	7.723164	5.877025	-	-
Point37	5.127712	7.074209	5.724717	6.476062
Point38	8.050424	8.138876	10.83773	8.557933
Point39	5.915478	5.337638	9.908732	7.695535
Point40	7.68689	7.627013	13.18089	8.316576
Point41	3.0828	3.86022	5.616298	7.369519
Point42	5.790631	13.5991	12.52383	4.659003
Point43	16.47407	3.634466	16.69955	8.082533

Point44	3.908581	10.16195	9.758653	6.9531
Point45	5.281038	6.487417	8.063841	6.27623
Point46	-	-	-	-
Point47	3.399196	8.19108	11.35099	8.053604
Point48	4.503314	7.463935	12.49008	8.199568
Point49	13.4982	4.009211	12.13487	17.41005
Point50	5.072309	4.9976	9.849587	-
Point51	6.249641	7.995099	12.70417	6.352084
Point52	5.306517	4.206766	20.80478	7.686301
Point53	-	-	-	-
Point54	3.971949	4.112882	2.632444	1.326056
Point55	6.235907	5.514806	7.542406	8.00769
Point56	4.996122	7.679908	-	8.805688
Point57	2.648634	2.435246	6.849607	2.840516
Point58	4.565134	4.325063	8.3505	6.883006
Point59	2.919733	4.122181	8.122605	4.608655
Point60	2.310302	3.767433	9.961145	5.362716
Point61	3.461073	9.495537	-	6.707175
Point62	5.881299	7.891641	7.95766	5.241042
Point63	3.064808	3.710327	6.523387	4.847569
Point64	-	3.929667	8.496998	6.68077
Point65	2.051108	4.566453	9.122788	4.489291
Point66	2.947415	5.554808	6.21245	8.266934
Point67	8.118018	5.976673	3.684038	5.914804
Point68	2.831894	6.856932	38.50012	0.577453
Point69	5.226973	2.345011	31.87837	6.785487
Point70	50.71023	3.85847	12.99226	7.62634
Point71	2.308618	9.505103	5.296594	5.115474
Point72	4.116443	3.925672	5.485768	6.599079
Point73	4.411652	5.076496	38.96015	6.91655
Point74	7.097879	7.781296	32.07923	7.62749
Point75	4.759033	8.320589	9.683558	9.90693
Point76	1.125387	2.071978	-	-
Point77	2.413616	5.684821	13.92464	5.927006
Point78	3.907628	4.841248	7.618982	4.981835
Point79	1.344954	4.378592	9.389402	4.365104
Point80	5.079258	4.924106	12.29974	9.122408
Point81	10.0506	9.92216	12.45473	12.61924
Point82	11.50981	11.95516	21.21186	12.32967
Point83	9.411364	8.768008	14.94968	9.153167
Point84	17.51974	-	9.01702	17.51974
Point85	8.511343	10.23562	13.58266	10.89984
Point86	7.036241	-	14.55431	-
Point87	5.6812	10.20601	17.88966	12.09913
Point88	5.320329	9.599783	17.73753	8.218451
Point89	4.309682	9.844991	15.11531	12.16405

Point90	5.219729	10.88625	14.57526	6.029338
Point91	4.759141	5.847904	5.461701	7.739031

Matlab code

Calculating hydraulic conductivity

```
%% Code for analyzing the transient infiltration data using:
    %1. method 2 by Zhang(1998)
    %2. Steady state solution,using the mean of the 4 last infiltration
        %rates as steady state infiltration
    %3. The differential linearization proposed by Vandervaere(1997) to
        %obtain parameters for the two parameter equation: I=C1*sqrt(t)+C2t

    %with compensation for new data in excel files causing need to to
change variable
    %names and removal of unnecesseray data in the start, causing problems
    %with the differential linearization
close all
%% Changing variable names
    h1=K1z;
    t1=VarName2;
    I1=VarName4;
    h2=K1d;
    t2=L;
    I2=K2s;

%% Curve fitting
rt=0.044/2;  %radius of supply tower
rd=0.20/2;     %radius of disc
    %measurement 1
        %load data1 %loads the datafile from the 1st transient flow
recording
        %with h=h1
        h1=h1*(-1);      %specifies the used tension
        h1(isnan(h1)) = [];%removes NaN associated with the reading
        t1=t1;   %specifies the time variable
        t1(isnan(t1)) = [];%removes NaN associated with the reading
        I1=I1;    %specifies the infiltration variable
        I1(isnan(I1)) = [];%removes NaN associated with the reading

        EQ=fittype({'x^(1/2)','x'});%specifies the function that will be
fitted to the data
        CF1=fit(t1,I1,EQ);             %fits the equation above to the data
        C1=coeffvalues(CF1);       %creates a coefficient vector
        C11=C1(1);                %coefficient C1, for the first
measurement, as in the Zhang method 2
        C12=C1(2);                %coefficient C2, for the first
measurement, as in the Zhang method 2

    %measurement 2
        %load data2 %loads the datafile from the 2nd transient flow
recording
        %with h=h2
        h2=h2*(-1);      %specifies the used tension
        h2(isnan(h2)) = [];%removes NaN associated with the reading
        t2=t2;   %specifies the time variable
        t2(isnan(t2)) = [];%removes NaN associated with the reading
        I2=I2;    %specifies the infiltration variable
        I2(isnan(I2)) = [];%removes NaN associated with the reading

        EQ2=fittype({'x^(1/2)','x'});%specifies the function that will be
fitted to the data
```

```
        CF2=fit(t2,I2,EQ2);             %fits the equation above to the
data
        C2=coeffvalues(CF2);       %creates a coefficient vector
        C21=C2(1);                %coefficient C1, for the second
measurement, as in the Zhang method 2
        C22=C2(2);                %coefficient C2, for the second
measurement, as in the Zhang method 2

%% calculating hydraulic conductivity and macroscopic capilarity length
        n=1;
        if length(I1)>=length(I2)    %arbittrary time used later
            n=(length(I2)-3);
        else
            n=(length(I1)-3)
        end
    %correction factors
        f1=0.5*(C11/C12)*t1(n).^(-1/2)+1; %correction factor 1 at an
arbitrary time
        f2=0.5*(C21/C22)*t2(n).^(-1/2)+1; %correction factor 2 at an
arbitrary time
        i1=0.5*C11*t1.^(-0.5)+C12;   %infiltration rate for measurement 1
        i1n=0.5*C11*t1(n)^(-0.5)+C12;%infiltration rate for first
measurement at an arbitrary time
        i2=0.5*C21*t1.^(-0.5)+C22;   %infiltration rate for measurement 2
        i2n=0.5*C21*t2(n)^(-0.5)+C22;%infiltration rate for second
measurement at an arbitrary time

    %macroscopic capilarity length
        Dh=h1-h2;           %difference in tension between the measurements
        Lz=Dh*(i1n*f2+i2n*f1)/(2*(i1n*f2-i2n*f1))%macroscopic capiliarity
length, Zhang

    %hydraulic conductivities
        r=0.20/2;        %specify radius of infiltrometer disc (D=0.2m)
        K1z=(i1n*(pi*(0.044/2)^2)/f1)/(pi*r^2+4*Lz*r)%hydraulic
conductivity for measurement 1, Zhang
        K2z=(i2n*(pi*(0.044/2)^2)/f2)/(pi*r^2+4*Lz*r)%hydraulic
conductivity for measurement 2, Zhang
%% steady state

                %part for loading data, only used if run solo without zhang
%         %with h=h1
%         h1=h1*(-1);      %specifies the used tension
%         h1(isnan(h1)) = [];%removes NaN associated with the reading
%         t1=t1;   %specifies the time variable
%         t1(isnan(t1)) = [];%removes NaN associated with the reading
%         I1=I1;    %specifies the infiltration variable
%         I1(isnan(I1)) = [];%removes NaN associated with the reading

        n=1;
        i1=1:4;
        for n=1:4;  %writing down the steady state assuming correct
measurement procedure(4 consequitive measurements with same rate)
        i1(n)=(I1(length(I1)-(4-n))-I1(length(I1)-(4-(n-
1))))/(t1(length(t1)-(4-n))-t1(length(t1)-(4-(n-1))));
        n=n+1;
        end

        Q1s=mean(i1)*rt^2*pi;    %flow at steady state assuming correct
measurement procedure(4 consequitive measurements with same rate)
```

```
        %part only for loading data, only used if run solo without zhang
%         %with h=h2
%         h2=h2*(-1);      %specifies the used tension
%         h2(isnan(h2)) = [];%removes NaN associated with the reading
%         t2=t2;   %specifies the time variable
%         t2(isnan(t2)) = [];%removes NaN associated with the reading
%         I2=I2;    %specifies the infiltration variable
%         I2(isnan(I2)) = [];%removes NaN associated with the reading

        n=1;
        i2=1:4;
        for n=1:4;  %writing down the steady state assuming correct
measurement procedure(4 consequitive measurements with same rate)
        i2(n)=(I2(length(I2)-(4-n))-I2(length(I2)-(4-(n-
1))))/(t2(length(t2)-(4-n))-t2(length(t2)-(4-(n-1))));
        n=n+1;
        end

        Q2s=mean(i2)*rt^2*pi;    %flow at steady state assuming correct
measurement procedure(4 consequitive measurements with same rate)

%calculations of values
        a=log(Q1s/Q2s)/(h1-h2);   %calculating alpha
        Ksat1=Q1s/((pi*rd^2)*exp(a*h1)*(1+4/(pi*rd*a)));
        Ksat2=Q2s/((pi*rd^2)*exp(a*h2)*(1+4/(pi*rd*a)));
        K1s=Ksat1*exp(a*h1)
        K2s=Ksat1*exp(a*h2)
%% Differentiated linearization+Zhang method 2
    %% measurement 1

        %for-loop for calculating d(I)/dsqrt(t), approximated by
        %Delta(I)/Delta(sqrt(t))
        i=1;
        dI1dVt1=[1:(length(I1)-1)]';    %declaring length of d(I)/dsqrt(t)
        Vt1=[1:(length(I1)-1)]';        %declaring length of sqrt(t)
        for i=1:(length(I1)-1)
            Vt1(i)=(sqrt(t1(i)*t1(i+1)))^(1/2);   %square root of t,
approximated with geometric mean between two measurements
            i=i+1;
        end

        for i=1:(length(I1)-1)
            %Vt1(i)=(sqrt(t1(i+1)*t1(i)))^(1/2);   %square root of t,
approximated with geometric mean between two measurements
            dI1dVt1(i)=(I1(i+1)-I1(i))/(sqrt(t1(i+1))-sqrt(t1(i)));
            i=i+1;
        end


    %% measurement 2

        %for-loop for calculating d(I)/dsqrt(t), approximated by
        %Delta(I)/Delta(sqrt(t))
        i=1;
        dI2dVt2=[1:(length(I2)-1)]';    %declaring length of d(I)/dsqrt(t)
        Vt2=[1:(length(I2)-1)]';        %declaring length of sqrt(t)
        for i=1:(length(I2)-1)
            Vt2(i)=(sqrt(t2(i+1)*t2(i)))^(1/2);   %square root of t,
approximated with geometric mean between two measurements
```

```
            dI2dVt2(i)=(I2(i+1)-I2(i))/(sqrt(t2(i+1))-sqrt(t2(i)));
            i=i+1;
        end

%% curve fitting
    %measurement1
        t1wo0=t1;      %modify the time variable[WithOut 0] to have
relevance to d(I)/dsqrt(t)
        t1wo0(1)=[];
        EQ=fittype({'1','2*x'});  %specifies the function that will be
fitted to the data
        CF1=fit(Vt1,dI1dVt1,EQ);         %fits the equation above to the
data
        C1=coeffvalues(CF1);            %creates a coefficient vector
        C11=C1(1);                %coefficient C1, for the first
measurement
        C12=C1(2);                %coefficient C2, for the first
measurement
    %measurement2
        t2wo0=t2;      %modify the time variable[WithOut 0] to have
relevance to d(I)/dsqrt(t)
        t2wo0(1)=[];
        CF2=fit(Vt2,dI2dVt2,EQ);         %fits the equation above to the
data
        C2=coeffvalues(CF2);            %creates a coefficient vector
        C21=C2(1);               %coefficient C1, for the second
measurement
        C22=C2(2);               %coefficient C2, for the second
measurement
%% confirmation and comparision by pointting
    %measurement 1
        point(t1,I1,['+','r']);
        hold on;
        point(Vt1.^2,C11*Vt1+C12*Vt1.^2,'b');
        Figure
        point(Vt1,dI1dVt1,'+')
        hold on
        point(Vt1,C11+2*C12*Vt1);
        xlabel('s^{1/2}');
        ylabel('m*s^{0.5}');
    %measurement 2
        Figure
        point(t2,I2,['+','r']);
        hold on;
        point(Vt2.^2,C21*Vt2+C22*Vt2.^2,'b');
        Figure
        point(Vt2,dI2dVt2,'+')
        hold on
        point(Vt2,C21+2*C22*Vt2);
        xlabel('s^{1/2}');
        ylabel('m*s^{0.5}');
%% calculating hydraulic conductivity and macroscopic capilarity length
    %correction factors
        f1=0.5*(C11/C12)*t1(n).^(-1/2)+1; %correction factor 1 at an
arbitrary time
        f2=0.5*(C21/C22)*t2(n).^(-1/2)+1; %correction factor 2 at an
arbitrary time
        i1=0.5*C11*t1.^(-0.5)+C12;   %infiltration rate for measurement 1
        i1n=0.5*C11*t1(n)^(-0.5)+C12;%infiltration rate for first
measurement at an arbitrary time
        i2=0.5*C21*t1.^(-0.5)+C22;   %infiltration rate for measurement 2
```

```
        i2n=0.5*C21*t2(n)^(-0.5)+C22;%infiltration rate for second
measurement at an arbitrary time

    %macroscopic capilarity length
        Dh=h1-h2;           %difference in tension between the measurements
        Ld=Dh*(i1n*f2+i2n*f1)/(2*(i1n*f2-i2n*f1))%macroscopic capiliarity
length, DL

    %hydraulic conductivities
        r=0.20/2;        %specify radius of infiltrometer disc (D=0.2m)
        K1d=(i1n*(pi*(0.044/2)^2)/f1)/(pi*r^2+4*Ld*r)%hydraulic
conductivity for measurement 1, DL
        K2d=(i2n*(pi*(0.044/2)^2)/f2)/(pi*r^2+4*Ld*r)%hydraulic
conductivity for measurement 2, DL
```

Statistics

Method I

```
% Script for making all the necessary graphs related to the statistics
%of the results of the Steady state method

probpoint('normal',K1s)
Figure
probpoint('lognormal',K1s)
Figure
probpoint('extreme value',K1s)
Figure
probpoint('normal',K2s)
Figure
probpoint('lognormal',K2s)
Figure
probpoint('extreme value',K2s)
m1=mean(K1s);
s1=std(K1s);
m1LOG=mean(log(K1s));
s1LOG=std(log(K1s));
m2=mean(K2s);
s2=std(K2s);
m2LOG=mean(log(K2s));
s2LOG=std(log(K2s));
Figure
x=[1:length(K1s)]';
n1=normpdf(K1s,m1,s1);

point(x,n1);
Figure
point(K1s,n1,'*');
n2=normpdf(K2s,m2,s2);
Figure
point(K2s,n2,'*');
```

Method II

```
%% Script for making all the necessary graphs related to the statistics
%of the results of the Differentiated Linearization(DL) method

probpoint('normal',K1z)
Figure
probpoint('lognormal',K1z)
Figure
probpoint('extreme value',K1z)
Figure
probpoint('normal',K2z)
Figure
probpoint('lognormal',K2z)
Figure
probpoint('extreme value',K2z)
m1=mean(K1z);
s1=std(K1z);
m1LOG=mean(log(K1z));
s1LOG=std(log(K1z));
m2=mean(K2z);
s2=std(K2z);
m2LOG=mean(log(K2z));
s2LOG=std(log(K2z));
Figure
x=[1:length(K1z)]';
n1=normpdf(K1z,m1,s1);

point(x,n1);
Figure
point(K1z,n1,'*');
n2=normpdf(K2z,m2,s2);
Figure
point(K2z,n2,'*');
```

Method III

```
%% Script for making all the necessary graphs related to the statistics
%of the results of the Differentiated Linearization(DL) method

probpoint('normal',K1dz)
Figure
probpoint('lognormal',K1dz)
Figure
probpoint('extreme value',K1dz)
Figure
probpoint('normal',K2dz)
Figure
probpoint('lognormal',K2dz)
Figure
probpoint('extreme value',K2dz)
m1=mean(K1dz);
s1=std(K1dz);
m1LOG=mean(log(K1dz));
s1LOG=std(log(K1dz));
m2=mean(K2dz);
s2=std(K2dz);
m2LOG=mean(log(K2dz));
s2LOG=std(log(K2dz));
Figure
x=[1:length(K1dz)]';
n1=normpdf(K1dz,m1,s1);
```

```
point(x,n1);
Figure
point(K1dz,n1,'*');
n2=normpdf(K2dz,m2,s2);
Figure
point(K2dz,n2,'*');
```

Soil moisture content

```
%% Script for making all the necessary graphs related to the statistics
%of the results of soil sample analysis
%% before experiment

S010=VarName2;
S010(isnan(S010)) = [];
S1020=VarName3;
S1020(isnan(S1020)) = [];
H010=VarName4;
H010(isnan(H010)) = [];
H1020=VarName5;
H1020(isnan(H1020)) = [];
probpoint('normal',S010)
Figure
probpoint('lognormal',S010)
Figure
probpoint('extreme value',S010)
Figure
probpoint('normal',S1020)
Figure
probpoint('lognormal',S1020)
Figure
probpoint('extreme value',S1020)
m1=mean(S010);
s1=std(S010);
m1LOG=mean(log(S010));
s1LOG=std(log(S010));
m2=mean(S1020);
s2=std(S1020);
m2LOG=mean(log(S1020));
s2LOG=std(log(S1020));
Figure
x=[1:length(S010)]';
n1=normpdf(S010,m1,s1);

point(x,n1);
Figure
point(S010,n1,'*');
n2=normpdf(S1020,m2,s2);
Figure
point(S1020,n2,'*');
%% after experiment

Figure
probpoint('normal',H010)
Figure
probpoint('lognormal',H010)
Figure
probpoint('extreme value',H010)
Figure
probpoint('normal',H1020)
```

```
Figure
probpoint('lognormal',H1020)
Figure
probpoint('extreme value',H1020)
m3=mean(H1020);
s3=std(H010);
m3LOG=mean(log(H010));
s3LOG=std(log(H010));
m4=mean(H1020);
s4=std(H1020);
m4LOG=mean(log(H1020));
s4LOG=std(log(H1020));
Figure
x=[1:length(H010)]';
n1=normpdf(H010,m1,s1);

point(x,n1);
Figure
point(H010,n1,'*');
n2=normpdf(H1020,m4,s4);
Figure
point(H1020,n2,'*');
```